




DISTRIBUTIONAL MATRIX COMPLETION VIA NEAREST NEIGHBORS IN THE WASSERSTEIN SPACE

BY JACOB FEITELBERG^{1,a} , KYUSEONG CHOI^{2,c} ,
ANISH AGARWAL^{1,b}, AND RAAZ DWIVEDI^{2,d} 

¹Industrial Engineering and Operations Research, Columbia University, ^ajef2182@columbia.edu; ^baa5194@columbia.edu

²Statistics and Data Science, Cornell Tech, Cornell University, ^ckc728@cornell.edu

³Operations Research and Information Engineering, Cornell Tech, Cornell University, ^drd597@cornell.edu

We study the problem of distributional matrix completion: Given a sparsely observed matrix of empirical distributions, we seek to impute the true distributions associated with both observed and unobserved matrix entries. This is a generalization of traditional matrix completion, where the observations per matrix entry are scalar-valued. To do so, we utilize tools from optimal transport to generalize the nearest neighbors method to the distributional setting. Under a suitable latent factor model on probability distributions, we establish that our method recovers the distributions in the Wasserstein metric. We demonstrate through simulations that our method (i) provides better distributional estimates for an entry compared to using observed samples for that entry alone, (ii) yields accurate estimates of distributional quantities such as standard deviation and value-at-risk, and (iii) inherently supports heteroscedastic distributions. In addition, we demonstrate our method on a real-world dataset of quarterly earnings prediction distributions. We also prove novel asymptotic results for Wasserstein barycenters over one-dimensional distributions.

1. Introduction. Matrix completion is the broad problem of imputing missing entries in a matrix. Algorithms for this problem have found widespread use in recommendation systems [31, 41, 45] used at companies such as Netflix, Amazon, and Meta, system identification [36], traffic sensing [22, 23, 53], device location sensing [39, 51], and patient-level predictions in healthcare [24, 52]. Although the theory and practice of matrix completion is thoroughly researched, there has been little to no work on matrix completion over distributions of numbers. We refer to this new problem as *distributional matrix completion*.

Distributions naturally model the case where multiple measurements are taken per matrix entry. To impute missing matrix entries using prior algorithms, the data analyst would first have to collapse multiple measurements into scalars by, for instance, averaging. However, by collapsing the distributions into scalars, we lose all information about other useful distributional properties, such as standard deviation, quantiles, and extrema. For example, in Fig. 1, we show three distributions with very different supports and other properties that all have the same means and variances. To alleviate this information loss problem, we propose and analyze a matrix completion algorithm to estimate entire distributions.

The goal of our paper is to explore how we can better exploit repeated measurements to (i) learn the underlying distributions associated with each matrix entry and (ii) better predict distributional quantities other than the mean such as median, variance, and value-at-risk. Distributional matrix completion’s difficulty stems from two information losses: we only observe a subset of the distributions, and for the distributions we do observe, we only have access to an empirical estimate of the distribution, not the true distributions. Additionally, distributions can exist in infinite-dimensional spaces, adding to the difficulty of extending the formal scalar matrix completion setup.

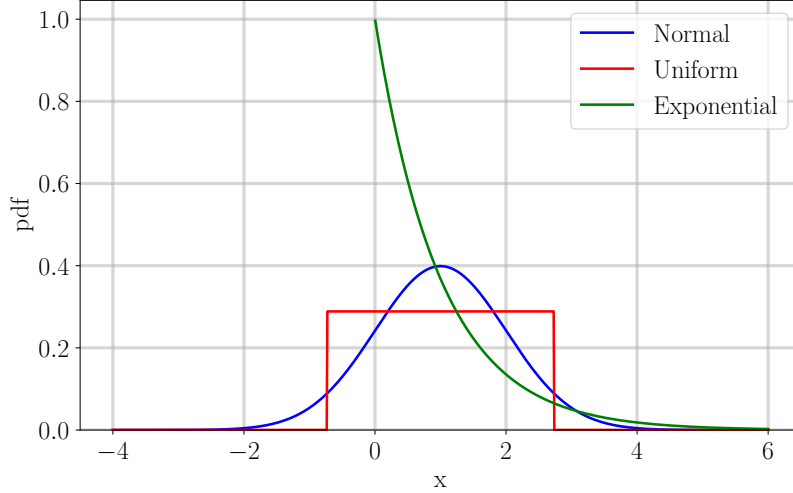


FIG 1. **Probability density functions (PDF's) of Gaussian, continuous uniform, and exponential distributions with the same mean ($\mu = 1$) and variance ($\sigma^2 = 1$)** While these distributions share first and second moments, they have very different properties. For instance, the Gaussian distribution's support is $(-\infty, \infty)$, the uniform distribution's support is $[-\sqrt{3}, \sqrt{3}]$, and the exponential distribution's support is $(0, \infty)$.

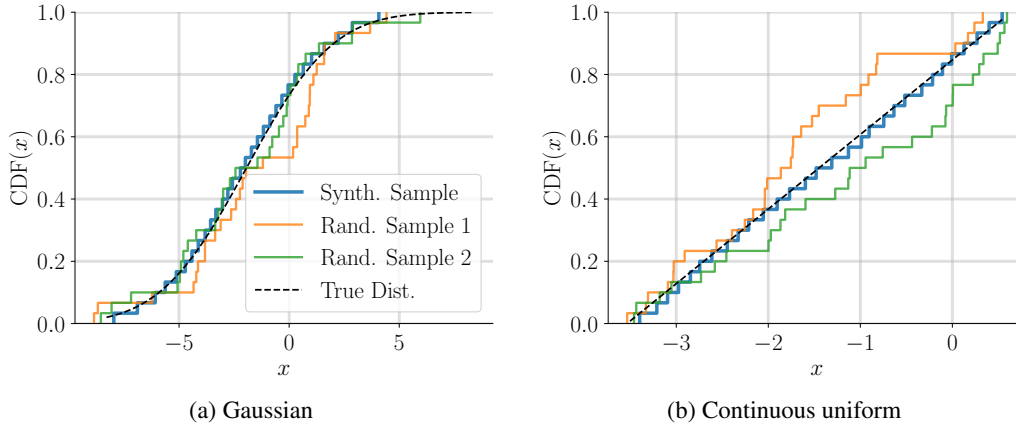


FIG 2. **Cumulative distribution functions (CDF's) of random empirical distributions vs. our synthetic distribution from matrix completion.** We simulate two distributional matrix completion examples, one with all empirical Gaussian distributions and one with empirical continuous uniform distributions. In both cases, only the matrix entry we seek to estimate is unobserved. Our method's synthetic distributions, shown in the thick blue lines, provide much better estimates of the true distribution's CDF, shown in black dotted lines, than simply using the empirical distribution of the observed matrix entries alone. See Sec. 6 for more details on our simulated tests.

We propose both a formal setup for distributional matrix completion and an estimation method to recover the unobserved true distribution per matrix entry. Using tools from optimal transport, our method is able to generate synthetic distributions that closely approximate the respective true distributions. Furthermore, perhaps surprisingly, the estimates consistently recover the true distributions more accurately compared to using just the empirical distribution for an observed matrix entry — see Figure 2. This allows for more accurate estimation of downstream distributional quantities such as variance or value-at-risk compared to simply using the observed empirical distribution.

1.1. *A motivating example: Quarterly earnings estimates.* To motivate distributional matrix completion with a real-world example, consider quarterly earnings estimates for public companies. Each fiscal quarter, public companies report their earnings (i.e. net income after taxes) for the previous quarter. Prior to this public release, analysts from various banks and other companies predict what they think the earnings will be for public companies. The distribution of predictions provides valuable insight for investors and traders into how a company is expected to perform and how much uncertainty there is in that predicted performance. On top of that, earnings estimates for one company often provide useful information on the performance of other companies. For instance, if earnings estimates for a part supplier to Nvidia suggest the part supplier is selling more components, then Nvidia might be selling more computer chips.

To systematically compare earnings estimate distributions, the predictions can be grouped by company and fiscal quarter to create a matrix of predictions where each matrix entry has a distribution of earnings predictions. Earnings predictions for a company are by definition a distribution of numbers because multiple analysts provide predictions. However, the time-dependent nature of the data induces missing entries in our distributional matrix in two ways: (i) companies do not follow the same fiscal quarter schedule and (ii) analysts for a single company can release their predictions over a month apart.

Consider the case where we are predicting Amazon’s earnings estimates for the second fiscal quarter of 2012 ahead of time. This data is useful because analyst estimates directly affect market prices by changing earnings expectations. However, two months prior to the first company releasing its actual earnings results, only a handful of analysts have released their predictions for any company. In this quarter, though, Apple released earnings before Amazon, and Apple’s full distribution of earnings estimates is observed before Amazon’s distribution. So, we can use the earnings distribution for Apple and other companies to predict Amazon’s future earnings estimate distribution. We propose to do this systematically using distributional matrix completion where the matrix has companies along the columns and fiscal quarters along the rows. For our tests in Sec. 6.2, we utilize data from 2010 through 2024 (~ 60 rows) for around 2,000 public companies ($\sim 2,000$ columns) based in the U.S.

1.2. *Related work.* Our work seeks to bridge two disparate topics, matrix completion and optimal transport, in order to provide a way to estimate unobserved probability distributions. Here, we provide a brief overview of the relevant literature in both areas.

Matrix completion. There are numerous algorithms for matrix completion that broadly fall into two categories: empirical risk minimization (ERM) and matching. Empirical risk minimization (ERM) methods seek to minimize both the distance between estimated matrix entries and observed matrix entries along with a regularization term [3, 11]. The regularizer seeks to prioritize less complex matrices and is sometimes replaced with a hard constraint, such as the matrix being low-rank [16]. Matching methods, or nearest neighbor methods, are popular for large-scale recommendation systems due to their simplicity and scalability [21, 32]. These algorithms estimate a missing entry by finding "similar" rows (users) or columns (items) and then use their average as the estimate for a missing entry. These algorithms not only work well in practice, but have been shown to have strong theoretical properties under suitable latent-factor models [25, 35]. To implement matching methods, one needs to generalize a notion of similarity and averaging between matrix entries to when they are distributions. We show how we do this in Sec. 3. The matrix completion literature has also grown to include noisy matrix completion [12, 35], panel data settings for causal inference [3, 25], and even matrix completion over more exotic spaces such as finite fields [44]. These areas, though, still assume the matrix has scalar values.

Optimal transport. Optimal transport (OT), a field initially developed to solve logistics problems [38], provides efficient computational and theoretical tools to compute the distance between two probability distributions and the average between a collection of distributions. OT has found widespread use from areas such as shape and image registration [26] to systems control [15]. Most work in OT has focused on efficiently finding the map to transport one distribution to another at the lowest cost for a given cost function [33, 46]. In this paper, we focus on the 2-Wasserstein distance, which is the cost of transporting one distribution to another when the cost function is the Euclidean distance. The Wasserstein distance also lends itself well to calculating distributional barycenters (i.e. averages) [7, 9, 20].

Wasserstein barycenters preserve the geometric properties of the input distributions. For instance, the barycenter of multiple Gaussian distributions is also Gaussian, unlike a mixture of Gaussians [6]. While Wasserstein barycenters have a closed-form solution for one-dimensional distributions, they have been proven to be NP-Hard to calculate in high dimensions [4]. In classical optimal transport literature, it is assumed that distributions are known completely, instead of sampled. The statistics of OT, an area that has become increasingly popular, focuses on comparing how empirical distributions generated from samples differ from their respective true distributions [6, 27, 34]. In the setup studied in this paper, we only have access to the empirical distributions. Hence the sample-size convergence rates of empirical distributions to true distributions proven in [10] are of particular use for us. In this work, we provide novel asymptotic results on empirical distributions in the Wasserstein space.

To the best of our knowledge, we know of one previous work using tools from OT for estimating unobserved distributions in the matrix setting: [29] present a method for learning counterfactual distributions in a synthetic control setting [1] using a quantile-based generalization of the synthetic control method. They perform a regression over quantile functions to construct their estimate, whereas we use a nearest neighbors method. [29] also assumes a linear mapping between latent factors and distributions, whereas we allow our mapping to be nonlinear. They make assumptions similar to ours on the underlying distributions to establish their theoretical results such as each distribution’s density being differentiable and lower bounded by a positive constant. However, we assume additional regularity conditions, such as bounded support and continuous density functions on the distributions, which enable us to prove faster rates of decay for the error rate (Assum. 3).

1.3. Organization and notation. In Sec. 2, we propose a Lipschitz latent function model for matrix completion over the space of one-dimensional probability distributions. In Sec. 3, we provide a distributional nearest neighbor estimation method which utilizes the geometry of the 2-Wasserstein space. In Sec. 4, we provide asymptotic error bounds for our estimator and establish its consistency as the number of rows and columns of the matrix, and the number of samples for a given observed matrix entry grow. We also establish the asymptotic distribution for the error of the estimand. In Sec. 5, we prove our first main theorem and highlight our new results in optimal transport which have relevance outside of of this problem. In Sec. 6, we use simulations to empirically verify our theoretical error decay rates. We also demonstrate our method’s accuracy in estimating distributional quantities such as mean, standard deviation, and quantiles. In Sec. 6.2, we demonstrate our method on the real-world earnings estimates example introduced in Sec. 1.1. Finally, in Sec. 7, we conclude and discuss future research directions.

Notation. We refer to a probability measure μ ’s cumulative distribution function as F_μ , its quantile function as F_μ^{-1} , and its density function as f_μ . For a generic function g of two parameters n and m , we write $g(n, m) = \mathcal{O}(h(n, m))$ if there exist positive constants c , n_0 , and m_0 such that for all $n \geq n_0$ and $m \geq m_0$, $g(n, m) \leq c h(n, m)$ [18]. We write $\tilde{\mathcal{O}}$ to hide any logarithmic factors of the function parameters. We write $X_n = \mathcal{O}_p(a_b)$ when X_n/a_b is

bounded in probability. We write $X_n = o_p(a_b)$ when X_n/a_b converges to 0 in probability. We denote the set $\{1, \dots, m\}$ as $[m]$. We denote the (i, j) -th entry of a matrix M as M_{ij} . When referring to a function g (e.g., cumulative distribution function, quantile function) of the empirical distribution from samples $\mathbf{X} = \{x_1, \dots, x_n\}$, we write $g_{\mathbf{X}}$. We abbreviate the term *almost surely* to *a.s.* and write $\stackrel{d}{=}$ to denote equality in distribution. We use \triangleq to denote that we are defining a new symbol. We also denote two random variables X and Y as independent by writing $X \perp\!\!\!\perp Y$. Finally, in regards to our algorithm, we use the words *user* and *row* interchangeably. We do the same with the words *item* and *column*. This originates from the literature for recommendation systems which typically have users along rows and items along columns.

2. Setup and data-generating process. In this section, we describe the general setup of distributional matrix completion. We then review some necessary background on optimal transport, which is used in our error calculations and estimation procedure. We then propose a data-generating process (DGP) that allows us to provide an error bound and asymptotic distribution for our method in Sec. 4.

2.1. Problem setup and generic nearest neighbors. In our setup, we analyze a partially observed $N + 1$ by $M + 1$ matrix, denoted Y , where each observed matrix entry contains an array of scalars; we add 1 to the matrix size to simplify the notation in our main theorem.. Within each matrix entry, Y_{ij} , the scalars are assumed to be drawn independently and identically (i.i.d.) according to some law μ_{ij} . For each matrix entry in a column j , we assume that number of samples is n_j . However, our algorithm and theoretical guarantees can easily generalize to unequally sized arrays within columns. If a matrix entry (i, j) is observed, then we denote the samples in that matrix entry as $\{y_{ij,k}\}_{k=1}^{n_j} \sim \mu_{ij}$. Note that for observed entries, we only have access to empirical data, not the true distribution. Using the observed empirical distributions, our goal is to estimate the true distributions, μ_{ij} , of the unobserved and observed matrix entries, i.e., for all rows and columns.

Missingness.. Let A be an $N + 1$ by $M + 1$ binary matrix representing which entries are observed and which are not. Then, we have

$$\text{for } i \in [N + 1], j \in [M + 1]: \quad Y_{ij} = \begin{cases} [y_{ij,1}, \dots, y_{ij,n_j}] & \text{if } A_{ij} = 1 \\ \text{missing} & \text{if } A_{ij} = 0 \end{cases}$$

where $\{y_{ij,k}\}_{k=1}^{n_j} \sim \mu_{ij}$.

Next, we outline the generic nearest neighbors algorithm that we generalize to solve distributional matrix completion.

Generic user-user scalar nearest neighbors algorithm.. The nearest neighbors algorithm requires a distance threshold, η , to define a neighborhood. The nearest neighbors algorithm then proceeds in two main steps impute a matrix entry (i, j) :

Step 1: Find the set of nearest neighbors for row i .

For each other row $u \neq i$ where $A_{uj} = 1$, define the columns that are observed in both rows i and u as

$$\mathcal{C}_{iu} \triangleq \{v \in [M + 1] \setminus \{j\} : A_{iv} = 1, A_{uv} = 1\}.$$

Then, find the average distance between the row i and row u as:

$$(1) \quad \rho_{iu} \triangleq \begin{cases} |\mathcal{C}_{iu}|^{-1} \sum_{v \in \mathcal{C}_{iu}} (Y_{iv} - Y_{uv})^2 & \text{if } |\mathcal{C}_{iu}| \geq 1 \\ \infty & \text{if } |\mathcal{C}_{iu}| = 0. \end{cases}$$

Finally, define row i 's η -nearest neighbors as

$$\mathcal{N}_{i,\eta} \triangleq \{u \in [N+1] : A_{uj} = 1, \rho_{iu} \leq \eta\}.$$

Step 2: Find the average of the nearest neighbors in column j .

If $|\mathcal{N}_{i,\eta}| > 0$, then estimate the missing entry at (i, j) as

$$(2) \quad \hat{Y}_{ij} = \frac{1}{|\mathcal{N}_{i,\eta}|} \sum_{u \in \mathcal{N}_{i,\eta}} Y_{uj}.$$

If we found no nearest neighbors, then return we could not find any neighbors for row i .

Step 1 finds rows which have matrix values close to the observed entries in the same row we are trying to estimate in. It then defines the nearest neighbors as the rows with distance below η . Step 2 returns the average of the nearest neighbors, $\mathcal{N}_{i,\eta}$, in column j . To generalize the nearest neighbors method from scalar matrix completion to the distributional setting, we need to provide distributional analogs of (1) and (2), i.e., we require a notion of *distance* and *average* in the probability distribution space. While there are many distributional distances such as total variation and Kullback–Leibler divergence, we utilize the Wasserstein distance and barycenter from optimal transport for this new setting as our notion of *distance* and *average*, respectively. It remains an interesting line of future research to explore the statistical and computational properties of other distributional distances.

Note that in this paper, we analyze user-user nearest neighbors. However, our work can be easily extended to user-item or item-item nearest neighbors. In item-item nearest neighbors, distances are calculated between columns and averages are taken over rows. In user-item nearest neighbors, distance and averages are taken both over rows and columns. See [25] for an example of how a user-item nearest neighbors algorithm is used to construct a doubly-robust estimator.

2.2. Distributional nearest neighbor similarity via Wasserstein distance. The Wasserstein distance is a natural choice for distributional nearest neighbors because (i) it satisfies the properties of a metric, (ii) it has a closed-form solution in the one-dimensional case, and (iii) it behaves well when distributions do not share supports. For instance, for total variation, denoted TV , $\text{TV}(U(0, 1), U(2, 3)) = \text{TV}(U(0, 1), U(4, 5)) = 1$ because these continuous uniform distributions do not share supports. The 2-Wasserstein distance, denoted W_2 , however, has $W_2(U(0, 1), U(2, 3)) < W_2(U(0, 1), U(4, 5))$. For other examples of the Wasserstein distance's useful geometric properties, see [49].

In the one-dimensional setting, the 2-Wasserstein distance can be written as an L^2 norm between quantile functions: For two probability measures on \mathbb{R} , μ and ν with finite second moment, we have [6, Eq. 2]

$$(3) \quad W_2(\mu, \nu) = \left(\int_0^1 |F_\mu^{-1}(x) - F_\nu^{-1}(x)|^2 dx \right)^{1/2} = \|F_\mu^{-1} - F_\nu^{-1}\|_{L^2(0,1)}$$

where F_μ^{-1} and F_ν^{-1} are the respective quantile functions of μ and ν . For empirical distributions μ_n and ν_n with the same number of samples, n , generated from samples $\{X_i\}_{i=1}^n$ and $\{Y_i\}_{i=1}^n$, respectively, we have a simpler formula [10, Lemma 4.2]:

$$(4) \quad W_2(\mu_n, \nu_n) = \left(\frac{1}{n} \sum_{i=1}^n (X^{(i)} - Y^{(i)})^2 \right)^{1/2}$$

where $X^{(i)}$ and $Y^{(i)}$ are the i -th order statistic of their respective empirical distributions μ_n and ν_n . Thus, the Wasserstein distance can be calculated in $\mathcal{O}(n \log(n))$ time between any

two empirical distributions with the same number of samples, n , with the asymptotic runtime being dominated by the sorting operation. Note that we interchangeably use “Wasserstein” and “2-Wasserstein” as we only consider the 2-Wasserstein distance in this work. We denote $W_2(\mathbb{R})$, the *Wasserstein space*, as the space of one-dimensional probability distributions on \mathbb{R} with finite second moment equipped with the 2-Wasserstein metric.

2.3. Distributional nearest neighbor averaging via Wasserstein barycenter. Consider the following probability distributions: $\mu_1, \dots, \mu_N \in W_2(\mathbb{R})$. The Wasserstein barycenter is defined as the probability distribution μ that minimizes $\sum_{i=1}^N W_2^2(\mu, \mu_i)$, similar to how an average over scalars minimizes the sum of the squared distance to each scalar. The Wasserstein barycenter also has a simple closed-form solution as the measure with quantile function [6, Eq. 8]:

$$(5) \quad F_\mu^{-1} = \frac{1}{N} \sum_{i=1}^N F_{\mu_i}^{-1}.$$

When each distribution μ_j is an empirical distribution derived from order statistics $\{X_{\mu_j}^{(i)}\}_{i=1}^n$, where $X_{\mu_j}^{(i)}$ is the i -th order statistic, then the Wasserstein barycenter’s distribution is an empirical distribution derived from order statistics given by [8, Section 2.4]:

$$X_\mu^{(i)} = \frac{1}{N} \sum_{j=1}^N X_{\mu_j}^{(i)}.$$

In other words, the Wasserstein barycenter is a discrete distribution with mass $1/n$ at each point $X_\mu^{(i)}$. To calculate the k -th order statistic of the Wasserstein barycenter, we first sort each distribution’s data into respective order statistics, and then average the k -th order statistics of the input distributions. Ordering each entry’s samples takes $\mathcal{O}(N \cdot n \log(n))$ time and calculating the order statistic average takes $\mathcal{O}(Nn)$ time. So, the runtime to calculate the barycenter is $\mathcal{O}(N \cdot n \log(n))$. The Wasserstein barycenter has several desirable properties: (i) it is computationally fast to calculate for empirical distributions, (ii) it behaves well with location-scale distributions such as Gaussian and continuous uniform, and (iii) it has a closed-form solution in the one-dimensional case which facilitates theoretical analysis. As an example of the Wasserstein barycenter’s geometric properties, it is shown in [6] that the barycenter of multiple Gaussian distributions is also Gaussian.

2.4. Data-generating process. Under no assumptions about the matrix, matrix completion is ill-posed since there are too many valid ways to impute missing entries. Therefore, matrix entries are often assumed to share some latent structure which reduces the degrees of freedom. One popular way to encode this latent structure is by assuming the matrix is low rank [16]. A more general framework to encode latent structure is given in [14] and contains low-rank matrices as a special case in the scalar setting [35, Sec. D]. We utilize the more general framework here as described below.

ASSUMPTION 1 (Lipschitz latent factor model on Wasserstein space). *Let the following latent structure hold: (i) There exists latent bounded metric spaces $(\mathcal{H}_{\text{row}}, d_{\text{row}}(\cdot, \cdot))$ and $(\mathcal{H}_{\text{col}}, d_{\text{col}}(\cdot, \cdot))$ for rows and columns, respectively, (ii) each row i has a latent vector $x_{\text{row}}^{(i)} \in \mathcal{H}_{\text{row}}$, each column j has a latent vector $x_{\text{col}}^{(j)} \in \mathcal{H}_{\text{col}}$, and (iii) there exists a function $f : \mathcal{H}_{\text{row}} \times \mathcal{H}_{\text{col}} \rightarrow W_2(\mathbb{R})$ such that for $i \in [N+1], j \in [M+1]$, $\mu_{ij} = f(x_{\text{row}}^{(i)}, x_{\text{col}}^{(j)})$. We assume that f is L -Lipschitz with respect to its row argument: For all $x_1, x_2 \in \mathcal{H}_{\text{row}}, y \in \mathcal{H}_{\text{col}}$, we have*

$$W_2(f(x_1, y), f(x_2, y)) \leq L d_{\text{row}}(x_1, x_2).$$

This assumption means that the true distributions vary smoothly in the Wasserstein space as we vary the respective latent row vectors. Thus, rows which are close together in the latent row space will have similar distributions within the same column. Since our method is a user-user nearest neighbors algorithm, we only require the latent function, f , to be Lipschitz with respect to the row argument. However, our model can be easily extended to user-item and item-item nearest neighbors by restricting f to be Lipschitz with respect to the column argument as well.

Before discussing two examples that satisfy Assum. 1 we must review the concept of *location-scale families* of distributions. A location-scale family of distributions is a set of distributions parameterized by a location parameter, $\alpha \in \mathbb{R}$, and a scale parameter, $\sigma \in \mathbb{R}_{\geq 0}$. For example, the Gaussian family of distributions is location-scale, as are the continuous and discrete uniform distribution families. Next, if μ is from a location-scale family, then for any random variable $X \sim \mu$ and for any $\sigma > 0$, $\alpha \in \mathbb{R}$, the random variable $Y \triangleq \sigma X + \alpha$ has a distribution from the same family as μ , and $F_Y^{-1} = \sigma F_X^{-1} + \alpha$. Thus, the quantile function of Y is linear in terms of the quantile function of X . This property facilitates analysis in the Wasserstein space because the quantile functions are used to calculate both the Wasserstein distance (3) and the Wasserstein barycenter (5). Note that one can interpret the noisy scalar matrix completion setup within this framework: if the noise in every matrix cell is from the same location-scale family, then this noisy scalar matrix completion case is covered under our distributional setup when we observe only one sample in each observed matrix cell.

Now, we can introduce two examples with defined latent row and column distributions which we utilize later to explain our theoretical results:

Example 1 (Homoscedastic location-scale). Let both the latent row and column factors be distributed uniformly over $[0, 1]^d$. For $x_{\text{row}}^{(i)}, x_{\text{col}}^{(j)} \in [0, 1]^d$, let the quantile function be $F_{\mu_{ij}}^{-1} = \sigma^2 F^{-1} + \langle x_{\text{row}}^{(i)}, x_{\text{col}}^{(j)} \rangle$ where F^{-1} is a quantile function corresponding to a distribution from a location-scale family.

Example 2 (Heteroscedastic location-scale). Let both the latent row and column factors be distributed uniformly over $[0, 1]$. For $x_{\text{row}}^{(i)}, x_{\text{col}}^{(j)} \in [0, 1]$, let the quantile function be $F_{\mu_{ij}}^{-1} = x_{\text{col}}^{(j)} F_{\mu}^{-1} + x_{\text{col}}^{(i)}$ for some quantile function F^{-1} from a location-scale family.

Ex. 1 induces a low-rank structure on the first moment of the distributions while keeping the scale parameter constant across matrix entries. Ex. 2 generates a matrix where each row has a different location and each column has a different scale. Ex. 1 satisfies the Lipschitz condition in Assum. 1 with $L = \sqrt{d}$, and Ex. 2 satisfies the Lipschitz condition with $L = 1$.

Next, we make an assumption about the missingness structure.

ASSUMPTION 2 (MCAR). *We assume the missing-completely-at-random (MCAR) case where each matrix entry's missingness $A_{ij} \sim \text{Bernoulli}(p)$, is i.i.d. across matrix entries, and is independent of the latent factors of the rows and columns.*

MCAR is a standard missingness pattern studied in the matrix completion literature, where the missingness is independent of both observed and unobserved factors. We believe that this MCAR assumption can be relaxed to the missing not-at-random (MNAR) case, but it is beyond the scope of this paper, and hence leave it as important future work.

3. Estimation method. In this section, we propose a generalization of scalar nearest neighbors to the distributional setting. As discussed earlier, Nearest neighbors scales well to very large datasets often encountered in recommendation systems and panel-data settings, making it very popular in practice. On top of that, nearest neighbors only requires a notion of *distance* and *average* to be implemented, which makes it a suitable choice for our setting

with complex infinite-dimensional objects; in particular, using the notion of 2-Wasserstein distance and barycenter, which we discussed as natural choices for computing similarity and averaging for one-dimensional distributions. We detail the distributional nearest neighbor algorithm below.

3.1. Distributional user-user nearest neighbors method. The inputs to our method are a data matrix, Y , a masking matrix A , and a distance threshold parameter, $\eta \geq 0$. For each entry (i, j) , we calculate $\hat{\mu}_{ij}$ as an estimate of μ_{ij} . We propose a nearest neighbors (NN) method, denoted DIST-NN, for our setting below:

DIST-NN(Y, A, i, j, η):

Step 1: Find the set of nearest neighbors for row i .

For each other row $u \neq i$ where $A_{uj} = 1$, define the columns that are observed in both rows i and u as

$$\mathcal{C}_{iu} \triangleq \{v \in [M+1] \setminus \{j\} : A_{iv} = 1, A_{uv} = 1\}.$$

Then, find the average distance between the row i and row u as:

$$(6) \quad \rho_{iu} \triangleq \begin{cases} |\mathcal{C}_{iu}|^{-1} \sum_{v \in \mathcal{C}_{iu}} W_2^2(Y_{iv}, Y_{uv}) & \text{if } |\mathcal{C}_{iu}| \geq 1 \\ \infty & \text{if } |\mathcal{C}_{iu}| = 0. \end{cases}$$

Finally, define row i 's η -nearest neighbors as

$$(7) \quad \mathcal{N}_{i,\eta} \triangleq \{u \in [N+1] : A_{uj} = 1, \rho_{iu} \leq \eta\}.$$

Step 2: Find the Wasserstein barycenter of the nearest neighbors in column j .

If $|\mathcal{N}_{i,\eta}| > 0$, then estimate the quantile function of μ_{ij} as:

$$(8) \quad F_{\hat{\mu}_{ij}}^{-1} = \frac{1}{|\mathcal{N}_{i,\eta}|} \sum_{u \in \mathcal{N}_{i,\eta}} F_{Y_{uj}}^{-1}.$$

If we found no nearest neighbors, then return that we could not find any neighborhood for row i .

In step 1, we calculate pairwise Wasserstein distances between row i and every other row that is observed in column j to estimate row i 's neighbors, which we denote $\mathcal{N}_{i,\eta}$. Once we have row i 's neighbors, in step 2, we find the Wasserstein barycenter of the observed distributions in column j for the nearest neighbors. This barycenter can be calculated using its quantile function, which has a closed-form solution from (5). Next, we present our theoretical guarantees for DIST-NN.

4. Main results. In this section, we present our main results showing that under certain regularity conditions on the probability distributions, our nearest neighbors method produces estimates close to their respective true probability distributions with high probability.

4.1. Error decay rate. To state our main results, we require several regularity conditions on the underlying distributions.

DEFINITION 1 (Regular measure). We say that a measure ν with distribution function F and density f is regular if (i) F is twice-differentiable and continuous on (a, b) where $-\infty < a < b < \infty$, (ii) there exists a universal $C > 0$ such that for all $x \in (a, b)$, $f(x) \geq C$, (iii) ν has a finite second moment, (iv) $(F^{-1})'$ is L' -Lipschitz, (v) f is non-decreasing in a right-neighborhood of a and non-increasing in a left-neighborhood of b , and (vi)

$$(9) \quad \sup_{x \in (a,b)} \frac{F(x)(1-F(x))}{f^2(x)} |f'(x)| < 2.$$

ASSUMPTION 3 (Regularity conditions). *For $(i, j) \in [N + 1] \times [M + 1]$, the measure μ_{ij} is regular.*

All continuous uniform distributions automatically satisfy this regularity condition because their probability density functions are constant on their respective supports. However, since we assume that our densities are uniformly lower bounded and compact, Gaussian distributions do not satisfy Assum. 3. This is a common issue when analyzing the asymptotic behavior of the Wasserstein distance. See [37, Remark 1] for a detailed discussion. We do note, however, that truncated Gaussian distribution satisfies these regularity conditions. Furthermore, in our simulations in Sec. 6, we find that when we apply our method to a matrix of Gaussian distributions, the empirical error rates are close to what our theoretical guarantees predict even though Gaussian distributions are not regular. Finally, the right-hand side in (9) merely simplifies the analysis and can be raised without loss of generality to some $\gamma < \infty$.

We now provide our first result, the error rate of the estimate DIST-NN (proven in App. A).

THEOREM 1 (Rate of error decay for $\hat{\mu}_{ij}$). *Let Assums. 1 to 3 hold. Let $|\mathcal{N}_{i,\eta}|$ be the number of neighbors for row i with distance threshold η . Let N and $\{n_v\}_{v \neq j}$ be fixed. Without loss of generality, let $|\mathcal{N}_{i,\eta}| \geq 1$. Then, we have that as $n_j, M \rightarrow \infty$*

$$W_2^2(\hat{\mu}_{ij}, \mu_{ij}) = \mathcal{O}_p \left(\eta + \frac{1}{p\sqrt{M}} + \frac{1}{n_j |\mathcal{N}_{i,\eta}|} + \frac{\log^2 n_j}{n_j^2} \right).$$

Thm. 1 shows that each estimated distribution $\hat{\mu}_{ij}$ closely approximates its respective true distribution μ_{ij} asymptotically with high probability. The first two terms are due to the bias in estimating the distance between two rows' latent factors. The last two terms originate from the Wasserstein distance between the empirical and true distributions in column j . The term $p\sqrt{M}$ serves as a high-probability lower bound on the number of overlapping observed columns between two rows when calculating row distances in (6). The third and fourth terms originate from the Wasserstein distance between the empirical and true distributions in column j and how that error propagates through the Wasserstein barycenter calculation in (7).

There is an implicit tradeoff captured in Thm. 1 between reducing the distance threshold η and increasing the number of neighbors $|\mathcal{N}_{i,\eta}|$. To prove consistency in the data parameters alone, we require further conditions on the latent row and column spaces. Specifically, we prove consistency for Exs. 1 and 2 discussed previously in Sec. 2. In the following corollary, let $\tilde{\mathcal{O}}_p$ suppress logarithmic dependencies and constants besides (M, N, p, n_j, d) . Then, we have the bounds (proven in App. C):

COROLLARY 1 (Location-scale consistency). *Let Assums. 1 to 3 hold. Let p be fixed. For the columns besides j , $v \neq j$, let the number of samples per entry in those columns be fixed and define their minimum as n_{-j} . Let the dimension of the latent row and column spaces be d . Let $\eta = \Omega(\frac{1}{n_{-j}} + \sqrt{\frac{\log N}{Mp^2}})$. Then, we have*

(a) *For the setting in Ex. 1, we have as $n_j, N, M \rightarrow \infty$*

$$(10) \quad W_2^2(\hat{\mu}_{ij}, \mu_{ij}) = \tilde{\mathcal{O}}_p \left(\frac{1}{n_{-j}} + \frac{1}{p\sqrt{M}} + \frac{1}{n_j(Np)^{\frac{2}{d+2}}} + \frac{\log^2 n_j}{n_j^2} \right).$$

(b) *For the setting in Ex. 2, the same bound (10) applies with the latent dimension $d = 1$.*

Cor. 1 provides a high-probability consistency result using only data parameters and no longer relies on the distance threshold parameter η . The $1/n_{-j}$ term corresponds to a

lower bound on η which allows us to still guarantee a sufficient number of neighbors. The $(Np)^{2/(d+2)}$ term is a high-probability lower bound on the number of neighbors that holds as long as η satisfies its respective lower bound. The second and fourth terms play similar roles as discussed above in Thm. 1. Note that similar to other non-parametric nearest neighbor results such as [24, 25, 35], Cor. 1 suffers from the curse of dimensionality in the third term and provides worse scaling with N if d is large. However, unlike scalar nearest neighbors, our bound also improves by increasing the number of samples we collect per matrix entry instead of only relying on the number of neighbors growing.

Discussion on Thm. 1. We discuss several important aspects of our theoretical results such as important differences with scalar nearest neighbor guarantees as well as novel results for Wasserstein barycenters. First, the number of neighbors and rows do not both have to increase to infinity for the error to go to 0. This is because as n_j increases, we get a better estimate of the true distributions in the j -th column, and these true distributions can be used to more accurately construct μ_{ij} . This is in contrast to scalar nearest neighbor methods, [24, 25, 35], which require the number of neighbors to go to infinity to achieve consistency. If n_j is finite, then the error will be bounded away from 0 because the Wasserstein barycenter of empirical distributions is a quantization of the Wasserstein barycenter of the true barycenter distribution. This is empirically shown in our simulations and follows from the definition of the Wasserstein barycenter of empirical distributions shown in (4). This is captured in the $\log^2 n_j / n_j^2$ term, which stems from the uniform error between an empirical quantile function and its respective true quantile function.

4.2. Asymptotic normality of quantiles. Before stating our next result, we define a new function from $[0, 1]$ to \mathbb{R} parameterized by a neighborhood $\mathcal{N}_{i,\eta}$ in column j :

$$(11) \quad \sigma_{\mathcal{N}_{i,\eta}}^2(t) \triangleq \frac{1}{|\mathcal{N}_{i,\eta}|} \sum_{u \in \mathcal{N}_{i,\eta}} \frac{t - t^2}{f_{\mu_{uj}}^2(F_{\mu_{uj}}^{-1}(t))}.$$

One can interpret this function as an analog of the variance term from the one-dimensional central limit theorem to the space of quantile functions. With this, we establish the following asymptotic normality result for any quantile of our estimator (proven in App. B):

THEOREM 2 (Asymptotic normality of $F_{\hat{\mu}_{ij}}^{-1}(t)$). *Let Assums. 1 to 3 hold. Let the sequence $\{n_{j,M}, N_M, \eta_M, \mathcal{N}_{i,\eta_M}\}_{M=1}^\infty$ satisfy*

$$(12) \quad \sqrt{|\mathcal{N}_{i,\eta_M}|} \frac{\log n_{j,M}}{\sqrt{n_{j,M}}} = o_p(1), \quad \text{and} \quad n_{j,M} |\mathcal{N}_{i,\eta_M}| \left(\eta_M + \frac{\log(2N_M)}{Mp^2} \right) = o_p(1).$$

Then, we have that for almost all $t \in (0, 1)$

$$(13) \quad \frac{\sqrt{n_{j,M} |\mathcal{N}_{i,\eta_M}|}}{\sigma_{\mathcal{N}_{i,\eta_M}}(t)} (F_{\hat{\mu}_{ij}}^{-1}(t) - F_{\mu_{ij}}^{-1}(t)) \xrightarrow{d} \mathcal{N}(0, 1) \quad \text{as} \quad M \rightarrow \infty.$$

The two regularity conditions in (12) ensure that the data and algorithmic parameters scale in a way that ensures asymptotic normality. The first condition requires the number of samples per entry in column j , n_j grows fast relative to the number of neighbors, $|\mathcal{N}_{i,\eta_M}|$. Each distribution used in the barycenter calculation is observed with some error because we only see a finite number of samples per matrix entry. This error propagates through the barycenter calculation, and thus this condition is required to control that error propagation. The second condition requires that the bias in estimating the distance between row latent factors goes to 0 faster than the the product $n_j |\mathcal{N}_{i,\eta_M}|$. This bias contributes to our error in estimating

the neighborhood set of a row, which propagates through our barycenter calculation. Thus, similar to the first condition, we require that the bias goes to 0 at a reasonable rate. Note that similar to Thm. 1, this result does not require the number of neighbors to grow to ∞ . However, this result is invalid if the number of neighbors is 0.

COROLLARY 2 (Location-scale asymptotic normality of $F_{\bar{\mu}_{ij}}^{-1}(t)$). *Let Assums. 1 to 3 hold. Let p be fixed. For the columns besides j , $v \neq j$, let the number of samples per entry in those columns be fixed and define their minimum as n_{-j} . Let the dimension of the latent row and column spaces be d . Consider the sequence $\{n_{j,M}, n_{-j,M}, N_M\}_{M=1}^\infty$. Let $\eta = \Omega\left(\frac{1}{n_{-j,M}} + \sqrt{\frac{\log N_M}{Mp^2}}\right)$. Then, we have:*

- (a) *For the setting in Ex. 1, (13) holds with $\mathcal{N}_{i,\eta}$ being any subset of the neighbors of size $\mathcal{O}(N_M^{2/(d+2)})$.*
- (b) *For the setting in Ex. 2, we have the same result, but with the latent dimension $d = 1$.*

Cor. 2 illustrates two settings in which an asymptotic normality result is applied, considering only the data parameters provided the distance threshold η satisfies a suitable scaling. The asymptotic normality result then holds for any subset of the neighborhood set that is of the size given in Cor. 2. The neighborhood set is guaranteed to satisfy the constraints with high probability, as proven in App. C. Notably, like in Thm. 2, we do not require the number of neighbors to diverge to infinity, and can in fact be capped at a constant value with the normality result still holding.

The asymptotic distributions in Thm. 2 and Cor. 2 allow us to provide approximate confidence bands for the quantile function of our estimate. Note that this is a pointwise, and not necessarily uniform, convergence in distribution. However, using Bonferroni’s correction [50], we can use this pointwise result to provide uniform confidence bands for the quantile function, as shown in Sec. 6. To exactly calculate $\sigma_{\mathcal{N}_{i,\eta_M}}(t)$, we require access to the true distributions of row i ’s neighborhood because we need the density and quantile functions for each neighbor. However, we show in Sec. 6 that a bootstrap estimate provides a reasonable approximation. Kernel density estimates (KDE’s) can also be used to estimate $\sigma_{\mathcal{N}_{i,\eta_M}}(t)$. See [37, Eq. (9)] for an example of using KDE’s to estimate quantities like $\sigma_{\mathcal{N}_{i,\eta}}(t)$. Next, we prove Thm. 1 and highlight an intermediate result which has applications in optimal transport.

5. Proof of Thm. 1. Here, we provide key parts of the proof of Thm. 1. A notable feature of our proof is a new result on distance between barycenter of a collection of measures and the barycenter of the empirical counterparts of that collection (Prop. 1), that can be of independent interest.

5.1. Overview of the proof of Thm. 1. We start with a basic decomposition of the error, and identify quantities that are akin to “bias” and “variance” in a typical decomposition of squared error. To do so, we first define $\bar{\mu}_{ij}$, the Wasserstein barycenter for the *true* distributions in the neighboring rows in column j :

$$\bar{\mu}_{ij} \triangleq \arg \min_{\mu} \sum_{u \in \mathcal{N}_{i,\eta}} W_2^2(\mu, \mu_{uj}).$$

From [6, Eq. 8], this minimum has a closed form solution in 1-dimension where $\bar{\mu}_{ij}$ is the measure with quantile function given by

$$F_{\bar{\mu}_{ij}}^{-1} = \frac{1}{|\mathcal{N}_{i,\eta}|} \sum_{u \in \mathcal{N}_{i,\eta}} F_{\mu_{uj}}^{-1}.$$

Next, we find that

$$\begin{aligned}
 (14) \quad W_2^2(\hat{\mu}_{ij}, \mu_{ij}) &\stackrel{(3)}{=} \left\| F_{\hat{\mu}_{ij}}^{-1} - F_{\mu_{ij}}^{-1} \right\|_{L^2(0,1)}^2 \\
 &= \left\| F_{\hat{\mu}_{ij}}^{-1} - F_{\bar{\mu}_{ij}}^{-1} + F_{\bar{\mu}_{ij}}^{-1} - F_{\mu_{ij}}^{-1} \right\|_{L^2(0,1)}^2 \\
 &\stackrel{(a)}{\leq} \left(\left\| F_{\hat{\mu}_{ij}}^{-1} - F_{\bar{\mu}_{ij}}^{-1} \right\|_{L^2(0,1)} + \left\| F_{\bar{\mu}_{ij}}^{-1} - F_{\mu_{ij}}^{-1} \right\|_{L^2(0,1)} \right)^2 \\
 (15) \quad &\stackrel{(b)}{\leq} 2 \left[\underbrace{W_2^2(\hat{\mu}_{ij}, \bar{\mu}_{ij})}_{\triangleq \mathcal{V}} + \underbrace{W_2^2(\bar{\mu}_{ij}, \mu_{ij})}_{\triangleq \mathcal{B}} \right],
 \end{aligned}$$

where (a) follows from the Minkowski inequality [30, Thm. 198] and (b) follows from the Cauchy-Schwarz inequality [30, Thm. 7]. We refer to \mathcal{B} as the “bias” because it captures the error from estimating the distance between rows. Similarly, we refer to \mathcal{V} as the “variance” because it captures the error from having a finite number of samples per cell. Next, we bound the terms \mathcal{B} and \mathcal{V} with two intermediate claims:

$$(16) \quad \mathcal{B} = W_2^2(\bar{\mu}_{ij}, \mu_{ij}) = \mathcal{O}_p(\eta + (Mp^2)^{-1/2}) \quad \text{as } M \rightarrow \infty, \quad \text{and}$$

$$(17) \quad \mathcal{V} = W_2^2(\hat{\mu}_{ij}, \bar{\mu}_{ij}) = \mathcal{O}_p\left(\frac{1}{n_j |\mathcal{N}_{i,\eta}|} + \frac{\log^2 n_j}{n_j^2}\right) \quad \text{as } n_j \rightarrow \infty.$$

which when put together with (15) yields the desired claim in Thm. 1.

The proof of (16) is provided in App. A.3, and it proceeds by using Minkowski’s inequality and Hoeffding concentration to generalize the proof from scalar setting to the distributional setting. The proof of (17) is technically more involved and relies on new results for Wasserstein barycenters, and we dedicate the next two subsections to contextualize our derivation with respect to prior work.

5.2. Prior additive error bound for empirical Wasserstein barycenter. To control the variance term $W_2^2(\hat{\mu}_{ij}, \bar{\mu}_{ij})$, one can leverage the rich literature on the Wasserstein distance bounds between empirical and true distributions for the Wasserstein barycenters in [6, 8–10, 34]. Specifically, consider a setting with k distributions $\{\mu_i\}_{i=1}^k$ with corresponding empirical distributions $\{\hat{\mu}_i\}_{i=1}^k$, where $\hat{\mu}_i$ denotes the empirical measure of n i.i.d. samples from μ_i . Let $\bar{\mu}$ and $\bar{\mu}_n$ denote the Wasserstein barycenters of the collections $\{\mu_i\}_{i=1}^k$ and $\{\hat{\mu}_i\}_{i=1}^k$. Then [6, Sec. 3.2.2] shows that

$$(18) \quad \mathbb{E}[W_2^2(\bar{\mu}, \bar{\mu}_n)] = \mathcal{O}\left(\frac{1}{k} + \frac{1}{n}\right)$$

where the expectation is taken over the randomness of sampling for each distribution. However, this scaling only provides an upper bound, e.g., when each μ_i is a uniform distribution on (possibly distinct but uniformly) bounded interval, then one can easily derive an improved and tight error rate (for completeness we state a formal result in App. D):

$$(19) \quad \mathbb{E}[W_2^2(\bar{\mu}, \bar{\mu}_n)] = \Theta\left(\frac{1}{nk} + \frac{1}{n^2}\right).$$

The scaling in (19) illustrates that depending on the number of measure k , the error rate scaling with respect to the number of samples n can range from n^{-1} to n^{-2} . This phenomenon

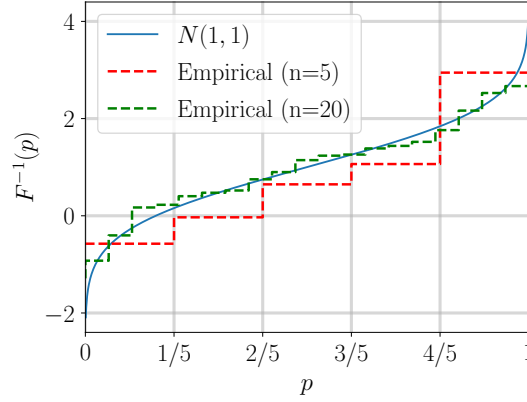


FIG 3. **True and empirical quantile functions for a Gaussian distribution with mean 1 and variance 1.** The red empirical distribution is generated from 5 random samples drawn from the Gaussian distribution. The green empirical distribution is generated from 20 random samples. Increasing the number of samples provides a closer approximation to the true quantile function.

is consistent with the empirical trends in Sec. 6 and Fig. 4, even though the distributions are not uniform. The remainder of our proof establishes that the improved error rate (19) in fact holds as long as each underlying distribution is regular.

5.3. New multiplicative error bound for empirical Wasserstein barycenter. Our next result, proven in Sec. 5.3.2, characterizes the convergence of empirical barycenter to the population barycenter as a function of both the sample size and the number of distributions:

PROPOSITION 1 (Convergence of the barycenter of empirical measures). *Consider a collection of regular (Def. 1) measures $\{\nu_j\}_{j=1}^k$ and let $\hat{\nu}_{j,n}$ denote the empirical distribution obtained from n i.i.d. samples from ν_j for each $j \in [k]$. Define the two barycenters*

$$\bar{\nu} \triangleq \arg \min_{\nu} \sum_{j=1}^k W_2^2(\nu, \nu_j) \quad \text{and} \quad \hat{\bar{\nu}}_n \triangleq \arg \min_{\nu} \sum_{j=1}^k W_2^2(\nu, \hat{\nu}_{j,n}).$$

Then we have

$$(20) \quad W_2^2(\hat{\bar{\nu}}_n, \bar{\nu}) = \mathcal{O}_p\left(\frac{1}{nk} + \frac{\log^2 n}{n^2}\right) \quad \text{as } n \rightarrow \infty,$$

uniformly with constants in $\mathcal{O}_p(\cdot)$ that depend neither on the set $\{\nu_j\}_{j=1}^k$ or its size k .

When compared to the additive error scaling $1/k + 1/n$ in (18) from prior work, the error scaling $1/(nk) + \log^2 n/n^2$ from Prop. 1 is a strict and significant improvement. Moreover, note that the error rate in (20) is uniform in two ways: (1) over the domain of the quantile function, $[0, 1]$, and (2) over the space of quantile functions that can be generated by the latent function f and the latent row and column spaces. Consequently, this rate can also be the random measures generated by the distribution over the latent spaces. In the context of our nearest neighbor guarantee, the former uniformity allows us to invoke the faster error rate for a fixed set of distributions (i.e., conditional on the neighboring distributions for a given distribution); the latter uniformity allows us to extend the argument to unconditionally, to a random collection of neighboring distributions.

Bridge between empirical Wasserstein barycenters and empirical quantile functions. To the best of our knowledge, Prop. 1 provides the tightest error bound for empirical Wasserstein barycenters approaching their respective true distributions. We prove this bound by bridging two research threads: error bounds for empirical Wasserstein barycenters and empirical quantile functions. In particular, the improved guarantee relies on two additional regularity conditions, standard in the literature on empirical quantile functions [19], imposed on the distributions in comparison to previous work in Wasserstein barycenters, namely parts (iv) and (v) in Def. 1. This bridge provides researchers in optimal transport with more tools and proof techniques to utilize when analyzing empirical Wasserstein barycenters.

With Prop. 1, we can now establish the bound (17) on the variance term \mathcal{V} from the decomposition (15):

5.3.1. *Proof of (17).* With Prop. 1 at hand, let us proceed to proving the claim (17). Our key step is to first condition on the latent row and column factors, so that the distributions in the neighborhood set $\mathcal{N}_{i,\eta}$ are fixed objects, and Prop. 1 can be applied. In the remainder of the proof, we abuse the notation and let Y_{uv} denote the samples in the matrix entry (u, v) regardless of whether (u, v) is observed or not.

For $u \in [N + 1]$, let I_u be the indicator random variable that $\rho_{iu} \leq \eta$. Recall the definition of the row-wise distance from (6):

$$\rho_{iu} \triangleq \begin{cases} |\mathcal{C}_{iu}|^{-1} \sum_{v \in \mathcal{C}_{iu}} W_2^2(Y_{iv}, Y_{uv}) & \text{if } |\mathcal{C}_{iu}| \geq 1 \\ \infty & \text{if } |\mathcal{C}_{iu}| = 0 \end{cases} \quad \text{where}$$

$$\mathcal{C}_{iu} \triangleq \{v \in [M + 1] \setminus \{j\} : A_{iv} = 1, A_{uv} = 1\}.$$

We have $Y_{uj} \perp\!\!\!\perp I_u$ since (i) the samples in column j are not used to calculate ρ_{iu} and (ii), from Assum. 2, the missingness of an entry is generated independently of the samples in that entry and all the latent factors. Next, we condition on the latent row and column factors \mathcal{U}_{row} and \mathcal{U}_{col} , making each distribution corresponding to the rows in the neighborhood set fixed.

Now, we are ready to apply Prop. 1, and then subsequently remove the conditioning. In column j , we assume that each observed matrix entry has n_j samples that are drawn i.i.d. from Sec. 2. Thus, we can apply Prop. 1 to the empirical distribution set $\{Y_{uj}\}_{u \in \mathcal{N}_{i,\eta}}$. Finally, since the bound in Prop. 1 is uniform with universal constants that do not depend on the distributions or $|\mathcal{N}_{i,\eta}|$, then we can remove the conditioning on the latent row and column factors \mathcal{U}_{row} and \mathcal{U}_{col} .

5.3.2. *Proof of Prop. 1: Convergence of the barycenter of empirical measures.* From [6, Eq. 8], the quantile functions of each barycenter has an explicit formula:

$$F_{\bar{\nu}}^{-1} = \frac{1}{k} \sum_{j=1}^k F_{\nu_j}^{-1} \quad \text{and} \quad F_{\hat{\bar{\nu}}}^{-1} = \frac{1}{k} \sum_{j=1}^k F_{\hat{\nu}_{j,n}}^{-1}.$$

So, we can write the Wasserstein distance between the two barycenters as:

$$\begin{aligned} (21) \quad W_2^2(\hat{\bar{\nu}}, \bar{\nu}) &\stackrel{(3)}{=} \|F_{\hat{\bar{\nu}}}^{-1} - F_{\bar{\nu}}^{-1}\|^2 \stackrel{(5)}{=} \left\| \frac{1}{k} \sum_{j=1}^k (F_{\hat{\nu}_{j,n}}^{-1} - F_{\nu_j}^{-1}) \right\|_{L^2(0,1)}^2 \\ &= \frac{1}{n} \left\| \frac{1}{k} \sum_{j=1}^k \sqrt{n} (F_{\hat{\nu}_{j,n}}^{-1} - F_{\nu_j}^{-1}) \right\|_{L^2(0,1)}^2 \\ &\triangleq \frac{1}{n} \left\| \frac{1}{k} \sum_{j=1}^k \sqrt{n} \hat{q}_{\nu_j, n} \right\|_{L^2(0,1)}^2, \end{aligned}$$

where we have defined $\hat{q}_{\nu_j,n} \triangleq \sqrt{n}(F_{\hat{\nu}_{j,n}}^{-1} - F_{\nu_j}^{-1})$ in the last step. To complete the proof, we next derive the asymptotic distribution of $\hat{q}_{\nu_j,n}$. While it is well known that $\hat{q}_{\nu_j,n}$ converges to a weighted Brownian bridge in distribution [43, Ch. 18],¹ the next lemma establishes a stronger result, namely a convergence in probability for the barycenters. Its proof builds on a strong uniform bound for empirical quantile functions provided in [19] and is provided in App. A.1.1.

LEMMA 1 (Approximation of barycenter). *Consider a collection of measures $\{\nu_j\}_{j=1}^k$ each of which satisfies Assum. 3. For each $j \in [k]$, let $\hat{\nu}_{j,n}$ denote the empirical distribution obtained from n i.i.d. samples from ν_j . Then, for each $j \in [k]$, there exists a sequence of standard Brownian bridges $\{\mathbb{B}_{j,n}\}_{n=1}^\infty$ and a universal constant c such that almost surely*

$$(22) \quad \frac{1}{n} \left\| \frac{1}{k} \sum_{j=1}^k \left(\sqrt{n}(F_{\hat{\nu}_{j,n}}^{-1} - F_{\nu_j}^{-1}) - \frac{\mathbb{B}_{j,n}}{f_j \circ F_j^{-1}} \right) \right\|_{L^2(0,1)}^2 \leq \frac{c \log^2 n}{n^2} = \mathcal{O}\left(\frac{\log^2 n}{n^2}\right).$$

Using the Brownian bridges appearing in Lem. 1, we obtain that

$$(23) \quad \begin{aligned} W_2^2(\hat{\nu}, \bar{\nu}) &\stackrel{(21)}{=} \frac{1}{n} \left\| \frac{1}{k} \sum_{j=1}^k \hat{q}_{\nu_j,n} \right\|_{L^2(0,1)}^2 \\ &= \frac{1}{n} \left\| \frac{1}{k} \sum_{j=1}^k \left(\hat{q}_{\nu_j,n} - \frac{\mathbb{B}_{j,n}}{f_{\nu_j} \circ F_{\nu_j}^{-1}} + \frac{\mathbb{B}_{j,n}}{f_{\nu_j} \circ F_{\nu_j}^{-1}} \right) \right\|_{L^2(0,1)}^2 \\ &\stackrel{(i)}{\leq} \frac{2}{n} \left\| \frac{1}{k} \sum_{j=1}^k \left(\hat{q}_{\nu_j,n} - \frac{\mathbb{B}_{j,n}}{f_{\nu_j} \circ F_{\nu_j}^{-1}} \right) \right\|_{L^2(0,1)}^2 + \frac{2}{n} \left\| \frac{1}{k} \sum_{j=1}^k \frac{\mathbb{B}_{j,n}}{f_{\nu_j} \circ F_{\nu_j}^{-1}} \right\|_{L^2(0,1)}^2, \end{aligned}$$

where (i) follows from applying Minkowski's inequality [30, Thm. 198] followed by the Cauchy-Schwarz inequality [30, Thm. 7]. While Lem. 1 establishes that the first term on the RHS of the above display is bounded almost surely, the next result provides tight control on the second term in probability.

LEMMA 2 (Norm of weighted average of Brownian bridges). *For each $j \in [k]$, let $\{\mathbb{B}_{j,n}\}_{n=1}^\infty$ be a sequence of independent standard Brownian bridges, and let $w_j : [0, 1] \rightarrow \mathbb{R}$ be L -Lipschitz. Then, we have*

$$\frac{1}{n} \left\| \frac{1}{k} \sum_{j=1}^k w_j \cdot \mathbb{B}_j \right\|_{L^2(0,1)}^2 = \mathcal{O}_p\left(\frac{1}{nk}\right).$$

We prove Lem. 2 in App. A.1.2 by showing that weighted sum of Brownian Bridges is a Gaussian process and then proving that this sum is uniformly bounded over all values of k . Finally, putting together (23) and Lems. 1 and 2, we obtain (20) as claimed in Prop. 1.

6. Numerical results. Here, we empirically show that DIST-NN is able to recover missing distributions using both simulations and the real-world example motivated in Sec. 1. With our simulations, we empirically show error decay rates similar to those proven in Sec. 4.

¹A stochastic process \mathbb{B} is a standard Brownian bridge if it is a Gaussian process where for $s, t \in (0, 1)$, $\mathbb{E}[\mathbb{B}(t)] = 0$, $\text{Cov}(\mathbb{B}(s), \mathbb{B}(t)) = \min(s, t) - st$. [42, Prop. 8.1.1]

6.1. Simulation results. We simulate the location-scale setting described in Ex. 2. The Python code to run our tests is available at our repository on [GitHub](#). Our method is also available for use in \mathbf{N}^2 ([GitHub](#)), a Python package which presents a unified interface for nearest neighbor-based matrix completion [17]. In these simulations, we let the sample size per matrix entry be n and thus equal across columns. In Fig. 4, we show error decay rates with respect to the number of samples n , the number of rows $N + 1$, and the product of n and the number of neighbors in the Gaussian location-scale case. We test the Gaussian case to connect with previous matrix completion literature, which primarily considers Sub-Gaussian noise. We also test our method on continuous uniform distributions in Figs. 2 and 5.

Each matrix entry is drawn from the same distribution family with only the location or scale being different between matrix entries like in Ex. 2. We draw locations from $Unif(-5, 5)$ and scales from $Unif(1, 5)$. *Without loss of generality*, our experiments have one missing entry in the matrix. Nearest neighbors estimates one entry at a time. Thus, if we can estimate one matrix entry, then we can estimate all of them.

We use cross-validation on observed matrix entries to choose our threshold parameter η . Specifically, if we are trying to estimate μ_{ij} , then we loop over each observed entry in row i , hold it out, and run our method to estimate that left out entry. We then compare our estimate with the observed entry. We choose the η that minimizes the squared Wasserstein distance between our estimate and the observed entry. Since this problem is nonlinear and nonconvex, we use the Tree of Parzen Estimators (TPE) method [5] to choose η . This method is a Bayesian optimization method that uses a Gaussian process to model the objective function. We use the Python library `hyperopt` to run TPE and used the standard settings with a maximum of 50 iterations.

Error with respect to number of samples, n . As shown in Fig. 4, as the number of samples, n , and the number of rows, $N + 1$, increase, our estimation error drops rapidly. For the error plot against the number of samples, we can see that our error decay rate improves from about $\mathcal{O}(n^{-1})$ to $\mathcal{O}(n^{-1.16})$ as the number of neighbors increases. This is supported by our theoretical result in Thm. 1 where as the number of neighbors increases, the dominant rate with respect to n becomes $\mathcal{O}(\log^2 n / n^2)$. We also see that the error rate power with respect to $n|\mathcal{N}_{i,\eta}|$ is around $\mathcal{O}((n|\mathcal{N}_{i,\eta}|)^{-0.8})$, which is close to the asymptotic bound of $\mathcal{O}((n|\mathcal{N}_{i,\eta}|)^{-1})$.

Error with respect to number of rows, N . For the error plot against the number of rows, we see that the error also drops rapidly with the number of rows. Again, we manage to achieve a better error decay rate than is predicted by our theoretical results. We also plot the expected error of an observed random sample in the dotted line to show that our method is able to produce an estimate that is far better than an observed random sample. Even for just 20 rows, our error is already significantly better than the expected error of a random sample. Thus, our synthetic sample is a much better estimate of the true distribution than an entry's random samples alone. We call this ability “denoising” because it mirrors the denoising ability of scalar nearest neighbors for noisy matrix completion.

Confidence bands. Using the results of Thm. 2, we can provide confidence bands for the quantiles of our estimates. In this simulated setting, we have access to the true distributions of the matrix entries we take a barycenter over. In practice, the $\sigma_{i,\mathcal{N}_{i,\eta}}$ quantity would need to be estimated. However, we show that a bootstrap estimate of the confidence bands using the empirical samples alone provides a good estimate of the true confidence bands.

In Fig. 5, we plot both the true and bootstrap confidence bands in the Gaussian and uniform location-scale cases. For our bootstrap method, we resample from both the individual neighboring distributions and resample over the neighbor set itself. We resample over samples and neighbors 10 times each for these simulations. In these settings, the bootstrap confidence

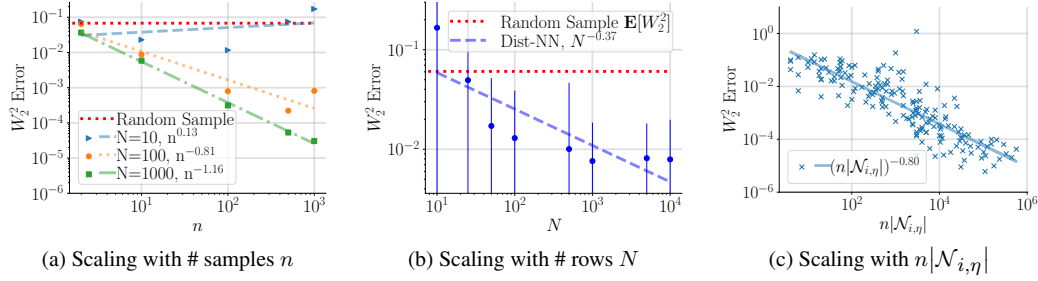


FIG 4. **Scaling of error with sample size n , number of rows N , and effective sample size $n|\mathcal{N}_{i,\eta}|$.** Every distribution in the matrix is a Gaussian distribution. Each row has an expected value sampled from $Unif(-5, 5)$. Each column has a standard deviation sampled from $Unif(1, 5)$. In plot (a), we set the number of columns to 30. We also require at least 2 nearest neighbors. In plots (a) and (b), we draw a random sample 100 times to estimate the expected error of a random sample in one matrix entry by itself. In plot (c), we set the number of samples to 500 and the number of columns to 10. We also cut the plot off on the top at 0.4 so that the lower error samples can be better visualized. We simulated each setting 50 times. Each curve is fitted using least squares to the power function $f(x) = ax^b$.

bands are more conservative than the asymptotic confidence bands. Note that we provide estimates for the Gaussian case even though the Gaussian distribution does not satisfy our assumption that the true distribution has a continuous quantile function on $[0, 1]$ because it is undefined at the boundary. This is why our estimate is poor around the boundary. However, the continuous uniform distribution satisfies our assumption. So, our estimate is much better around the boundary. Note that we provide estimates of simultaneous confidence bands as opposed to pointwise confidence bands for the quantile function, i.e., our confidence regions provide 95% coverage at each of the n points simultaneously. We provide simultaneous confidence bands using Bonferroni's correction [50] by dividing the confidence level, $\alpha = 0.05$, by the number of confidence intervals we plot, n .

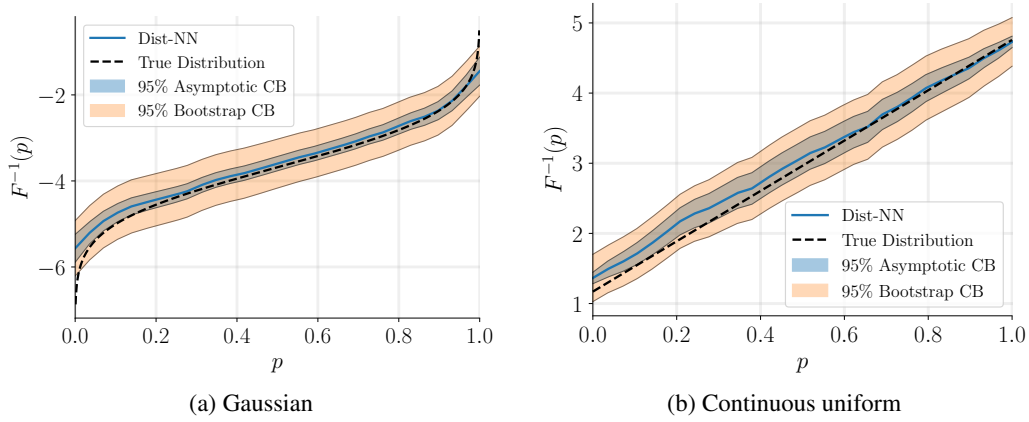


FIG 5. **Asymptotic and bootstrap simultaneous confidence bands for Gaussian and continuous uniform location-scale case.** The bootstrap confidence bands are more conservative than the bands provided by our asymptotic result. However, the bootstrap estimate resamples the neighboring distributions as well whereas the asymptotic one does not, which could make the bootstrap confidence bands more accurate. Also note that for the Gaussian case, our estimate is worse around $p = 0$ and $p = 1$. This is expected, because our theoretical guarantees rely on the true distribution being supported on a compact interval.

Denoising. We show the method’s denoising ability through empirical CDF’s in Fig. 2. This ability of nearest neighbors means that information can be shared across rows to achieve empirical distributions that are much closer to their respective true distributions than a random sample. This feature of our method is beneficial for downstream analysis since distributional quantities such as mean, variance, and value-at-risk can be estimated with a much higher accuracy than an isolated observed set of samples. Value-at-risk (VaR) is commonly used in financial modeling and is defined for $\alpha \in (0, 1)$ as $\text{VaR}_X(\alpha) = F_{-X}^{-1}(1 - \alpha)$ where X is a random variable and F_{-X}^{-1} is the quantile function of $-X$.

We show empirically that our method estimates distributional quantities well in Fig. 6. The synthetic sample produces estimates of the mean, standard deviation, value-at-risk, and median a lot closer to their respective true values than what an observed random sample baseline alone provides. Hence, running DIST-NN on observed distributions can potentially provide much better estimates of their true distributions than just using their random samples in isolation. Note that new distributional quantities can be calculated from our method’s output without re-running the entire estimation procedure because our method outputs a distribution. So, our method is estimating all of these quantities simultaneously.

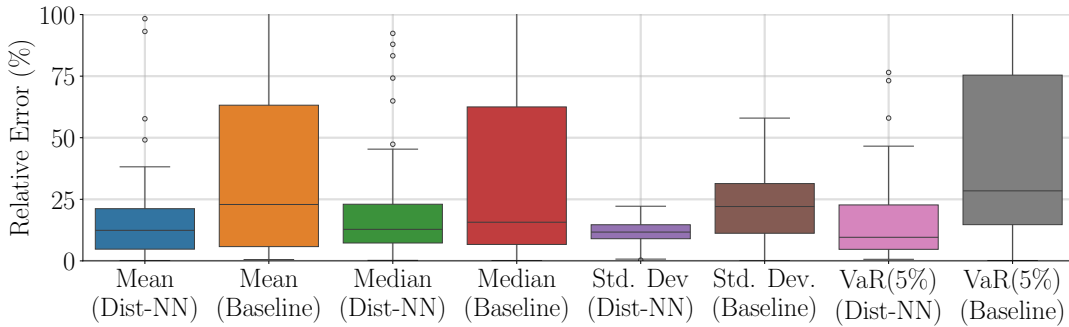


FIG 6. *Relative error for DIST-NN and a baseline of only using the distribution within a single matrix cell for estimating means, medians, standard deviations, and value-at-risk (VaR(5%)). We use the same Gaussian location-scale setup Fig. 4. DIST-NN is able to estimate all of these distributional quantities noticeably better the baseline. Thus, utilizing shared information across the matrix through DIST-NN helps to estimate all of these distributional quantities simultaneously. The box and whisker plots show the three quartiles in the shaded boxes, the range of the data, and any outliers. Note that we cut off the y-axis at 100% for readability.*

6.2. Real-world application: quarterly earnings estimates. We now demonstrate DIST-NN on the real-world example introduced in Sec. 1.1: imputing quarterly earnings estimate distributions for public companies. First, we review the importance of this dataset and how it is used in the real world. At the end of each fiscal quarter, public companies release their financial performance for the period. Prior to this public release, analysts from banks and other companies provide their own predictions for the quarterly results for each company that they track. These estimates are used by investors and traders to predict both company performance and gauge what the rest of the market believes about the company. Additionally, earnings estimates for one company provide useful information about other companies which are connected to it via business partnerships or by operating in the same market. For this empirical study, we focus on quarterly earnings (net income) estimates. The same procedure can be applied to yearly earnings or other financial metrics such as revenue.

Most investors, traders, and financial media companies partition earnings results and predictions by fiscal quarter. However, anyone analyzing earnings estimates between multiple

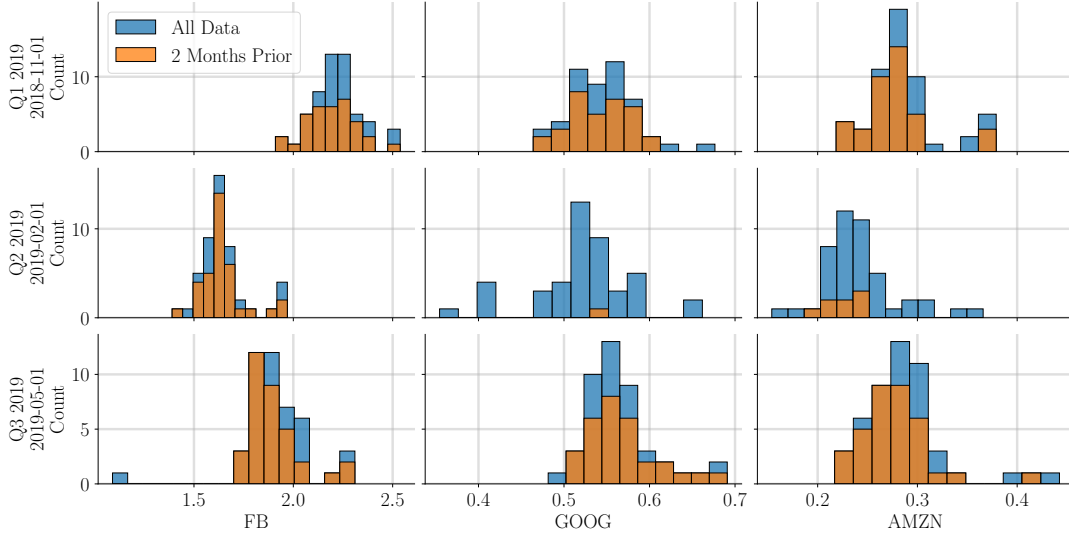


FIG 7. *Subset of analyst quarterly earnings estimates in the matrix format summarized as histograms. The companies here are Meta (Facebook), Google, and Amazon, and the quarters are Q1, Q2, and Q3 in 2019. We plot both the full histogram of earnings estimates available within the quarter for each company (blue) and the earnings estimates released 2 months before the first public announcements of actual results (orange). The date cutoff for the “2 Months Prior” data is in the description for the row (e.g. 2018-11-01 in the first row). Here, we observe the partial time-series based missingness where earnings estimates arrive on inconsistent schedules. For instance, Google has only one estimate in the second row by the cutoff date, but has most estimates in the third row by the cutoff date.*

companies in the same quarter will run into a *missing-data problem*: While some analysts release their predictions weeks ahead of the actual earnings release, other analysts wait until just one day beforehand. Thus, investors might only see a fraction of analyst predictions at any given date. On top of this, companies release their earnings results on inconsistent schedules. For instance, some quarters, Amazon releases earnings before Apple and other times vice versa. To remedy this time-dependent missing data problem, we propose to use DIST-NN to impute any missing (future) analyst estimate distributions. But first, we discuss where we obtain our data from and how we structure it into a matrix format.

We utilize analyst earnings estimates from the Institutional Brokers’ Estimate System (I/B/E/S) dataset via the Wharton Research Data Services (WRDS) platform.² I/B/E/S contains detailed data on analyst estimates for over 19,000 analysts across more than 23,400 companies with data as far back as 1976.³ We analyze a subset of this dataset: analyst estimates for publicly-traded companies based in the United States with the top 2,000 market capitalizations (combined value of a company’s outstanding common shares) from January, 2010 through December, 2024. We structure the data into a matrix with companies along the columns and quarter/year along the rows such as in Fig. 7. Since there is no accurate way of tracking estimates at the analyst level, combining estimates into empirical distributions is the most granular object to represent analyst estimates. We plot histograms using the Seaborn Python library [48].

²<https://wrds-www.wharton.upenn.edu/pages/get-data/ibes-thomson-reuters/>

³<https://www.lseg.com/en/data-analytics/financial-data/company-data/ibes-estimates>

We apply DIST-NN to this dataset to impute partially or completely missing distributions within a row that have not yet been fully observed. Within a quarter, if we choose an earlier date, there is more likely to be less data in each matrix cell because earnings estimates are made public on different dates. To test DIST-NN, we apply the following procedure: (1) Choose a date where data is missing, (2) determine which companies have very few of their earnings estimates in by the chosen date (less than 20% of their total estimates), (3) for each of these companies c , optimize a distance threshold η_c for DIST-NN using the previous quarters for that company, and (4) use the optimized η_c with DIST-NN to impute the missing entry. The returned barycenter for each (partially) missing company is constructed from the analyst estimate distributions from prior quarters. So, DIST-NN leverages other companies to compute the Wasserstein distance between distributions in the current quarter and distributions in previous quarters, and then computes the barycenter from similar previous quarters for the company of interest. After this procedure, we compare our imputed EPS estimates distribution with the full analyst estimate distributions reported at a future date. We also compare DIST-NN's performance with the distribution of estimates already seen by the chosen date (baseline). For example, in Fig. 7, the chosen dates for each row are 2018-11-01, 2019-02-01, and 2019-05-01. The baseline distributions are the orange histograms labeled "2 Months Prior," and the true distributions are blue and labeled "All Data."

In Fig. 8, we show numerically that DIST-NN is able to predict several distributional quantities of interest for partially missing distributions much better than only using the small amount of past data in one matrix cell, which we refer to as the baseline. DIST-NN particularly excels compared to the baseline for estimating $\text{VaR}(5\%)$, which makes sense because $\text{VaR}(5\%)$ is a quantile, which is a value targeted by using the Wasserstein geometry. In Fig. 9 we provide two examples that visually show how DIST-NN better approximates the true future distributions. These figures demonstrate that DIST-NN is able to predict future analyst estimate distributions by leveraging past data across both columns (companies) and rows (time). Our box and whisker plots are created using the Seaborn Python library [48].

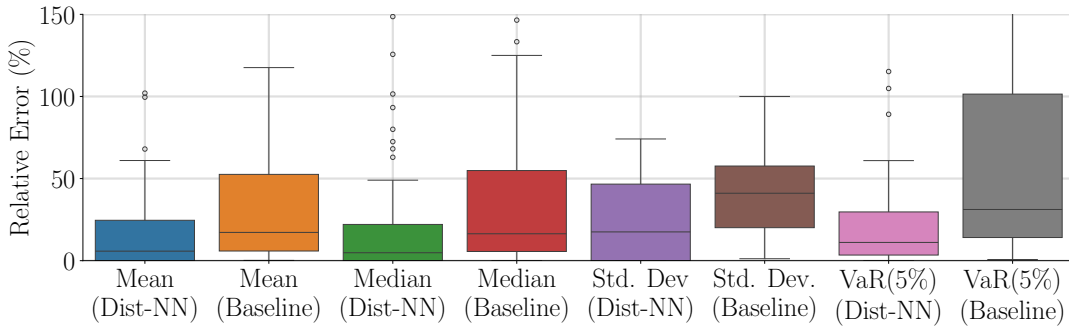


FIG 8. **Relative error for DIST-NN and the within-cell past data baseline in the I/B/E/S dataset for estimating means, medians, standard deviations, and value-at-risk numbers (VaR (5%)).** Here, we compare performance for estimating distributional quantities for missing (future) data for Q1 2019 using data from before November 1st, 2018. At this date, some quarterly estimates are available for Q1 2019, but not every estimate. The box and whisker plots show the three quartiles in the shaded boxes, the range of the data, and any outliers. We estimate distributions where less than 20% of the estimates are in using DIST-NN and compare with the baseline of using the raw data in a matrix cell alone before November 1st, 2018. DIST-NN is able to estimate distributional quantities much better than the baseline, especially for estimating $\text{VaR}(5\%)$. Note that we cut off the y-axis at 150% for readability.

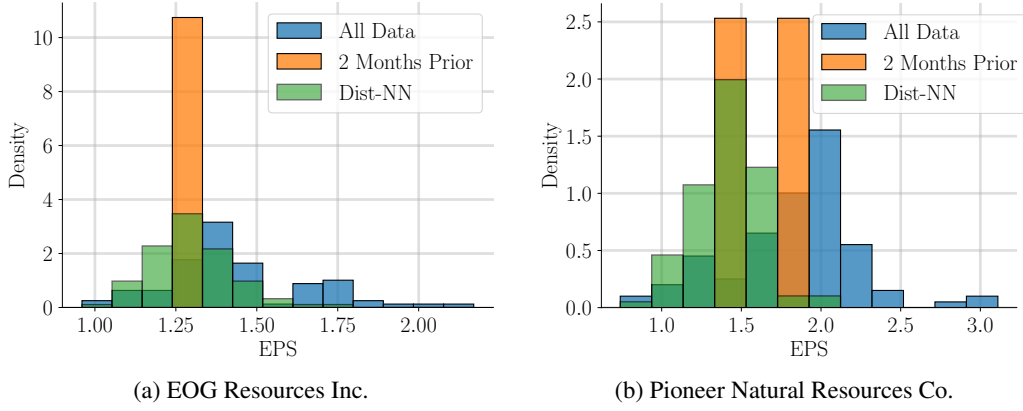


FIG 9. *Density plots of baseline past data and DIST-NN estimates along with the true future density plot. Here, we show two density plots of baseline and estimated distributions for two companies from the data used in Fig. 8. The histograms are normalized so that the total area covered is equal to 1, which is why we label the y-axis "density." We do this so that we can compare the distributions even if the past baseline data has fewer estimates. Clearly, the DIST-NN-estimated distributions capture the future true distributions better than the baseline distributions.*

7. Discussion. In this paper, we study the distributional matrix completion problem, where matrix entries are one-dimensional empirical distributions. We propose a distributional variant of the nearest neighbors method to solve this new problem using tools from optimal transport and prove theoretical asymptotic bounds and distributions for the estimate's error. Our simulations showcase the ability of DIST-NN to not only recover the unobserved distributions but also create synthetic distributions that are consistently closer to their true distributions than an observed random sample alone. We also demonstrate DIST-NN's performance on the I/B/E/S dataset of quarterly earnings estimates and show that we can impute future distributions.

DIST-NN can be modified into a user-item nearest neighbors algorithm where distances and averages are calculated across both rows and columns to create a doubly-robust estimator like in [25]. However, we leave this for future work to explore a double robust extension of the DIST-NN algorithm. Another important direction of future study is how to efficiently extend DIST-NN to higher-dimensional probability distributions because calculating Wasserstein barycenters suffers from the curse of dimensionality [4]. This slowdown is evident even on small 2D distributions such as grayscale images. One possible avenue is to restrict the class of probability distributions (see [34] for one such result). Second, it would be interesting to extend the theoretical analysis to the missing-not-at-random (MNAR) setting where the missingness is not independent of the observed data.

APPENDIX A: PROOF OF LEMMAS AND PROPOSITIONS FOR THM. 1

In this section, we provide detailed proofs for each supporting lemma and proposition used in the proof of Thm. 1 in Sec. 5.

A.1. Remaining parts from the proof of Prop. 1: Convergence of the barycenter of empirical measures. We now finish the proof of Prop. 1, by proving Lems. 1 and 2 in App. A.1.1 and A.1.2 respectively.

A.1.1. Proof of Lem. 1: Approximation of barycenter. First, we will apply the following theorem (note that we only restate the part of the theorem on Brownian bridges and not on Kiefer processes):

THEOREM A (Thm. 6 in [19]). *Consider a measure ν satisfying Assum. 3 and let $\hat{\nu}_n$ denote the empirical distribution obtained from n i.i.d. samples from ν . Then there exists a sequence of Brownian bridges $\mathbb{B}_1, \dots, \mathbb{B}_n$ such that*

$$\sup_{0 < t < 1} |f(F^{-1}(t))\sqrt{n}(F_{\hat{\nu}_n}^{-1}(t) - F_{\nu}^{-1}(t)) - \mathbb{B}_n(t)|$$

$$\stackrel{a.s.}{=} \begin{cases} \mathcal{O}(n^{-1/2} \log n) & \text{if } \gamma < 2 \\ \mathcal{O}(n^{-1/2} (\log \log n)^{\gamma} (\log n)^{(1+\epsilon)(\gamma-1)}) & \text{if } \gamma \geq 2, \end{cases}$$

where $\epsilon > 0$ is arbitrary.

From Assum. 3, we have $\gamma < 2$ for each distribution. So, we have that for each distribution ν_j and its respective approximation by a sequence of Brownian bridges, $(\mathbb{B}_{j,l})_{l=1}^n$,

$$\sup_{t \in (0,1)} |f_{\nu_j}(F_{\nu_j}^{-1}(t))\hat{q}_{\nu_j,n}(t) - \mathbb{B}_{j,n}(t)| \stackrel{a.s.}{=} \mathcal{O}\left(\frac{\log n}{\sqrt{n}}\right).$$

This result holds for each measure, but we need it to hold uniformly for any finite set of measures. Thus, we will unpack the proof of this theorem to show that it holds uniformly. Thm. A is proven by combining three theorems where u_n be the quantile process \hat{q}_n for a $Unif(0, 1)$ random variable:

THEOREM B (Thm. 1 in [19]). *If the uniform $(0,1)$ random variables U_1, U_2, \dots are defined on a rich enough probability space, then one can define, for each n , a Brownian bridge $\{\mathbb{B}_n(y) : 0 \leq y \leq 1\}$ on the same probability space such that, for all z , we have*

$$\mathbb{P}\left(\sup_{0 \leq y \leq 1} |u_n(y) - \mathbb{B}_n(y)| > n^{-1/2}(A \log n + z)\right) \leq B e^{-Cz}$$

for positive absolute constants A, B , and C ;

THEOREM C (Thm. 2 in [19]). *With $\delta_n = 25n^{-1} \log \log n$ we have*

$$(24) \quad \limsup_{n \rightarrow \infty} \sup_{\delta_n \leq y \leq 1 - \delta_n} (y(1-y) \log \log n)^{-1/2} |u_n(y)| \stackrel{a.s.}{\leq} 4; \quad \text{and}$$

THEOREM D (Thm. 3 in [19]). *Let X_1, X_2, \dots be i.i.d random variables with a continuous distribution function F which is also twice differentiable on (a, b) and $F' = f \neq 0$ on (a, b) . Let the quantile processes $\hat{q}_n(y)$ and respective $u_n(y)$ be defined in terms of the order statistics $X_{k:n}$ and $U_{k:n} = F(X_{k:n})$. Assume that for some $\gamma > 0$,*

$$\sup_{a < x < b} F(x)(1-F(x)) \left| \frac{f'(x)}{f^2(x)} \right| \leq \gamma,$$

and f is nondecreasing (increasing) on an interval to the right of a (to the left of b). Then, with δ_n as in Thm. C

$$\sup_{0 < y < 1} |f(F^{-1}(y))q_n(y) - u_n(y)|$$

$$\stackrel{a.s.}{=} \begin{cases} \mathcal{O}(n^{-1/2} \log \log n) & \text{if } \gamma < 1 \\ \mathcal{O}(n^{-1/2} (\log \log n)^2) & \text{if } \gamma = 1 \\ \mathcal{O}(n^{-1/2} (\log \log n)^{\gamma} (\log n)^{(1+\epsilon)(\gamma-1)}) & \text{if } \gamma > 1 \end{cases}$$

where $\epsilon > 0$ is arbitrary. The constants in the $\mathcal{O}(\cdot)$ are respectively, $2(\max(45, 25(2^{\gamma}/(1-\gamma)))) + 40\gamma 10^{\gamma}$ if $\gamma < 1$, 102 if $\gamma = 1$, and $2 \max(45, (2^{\gamma}/(\gamma-1))25^{\gamma})$ if $\gamma > 1$.

First, Thm. B can be easily extended to our setting using a simple union-bound:

$$\mathbb{P}\left(\sup_{i \in [k]} \sup_{0 \leq y \leq 1} |u_{n,i}(y) - \mathbb{B}_{n,i}(y)| > n^{-1/2}(A \log n + z)\right) \leq kBe^{-Cz}$$

So, as long as k does not grow faster than $\exp(z)$, this statement will still hold and we thus have

$$\sup_{i \in [k]} \sup_{0 \leq y \leq 1} |u_{n,i}(y) - \mathbb{B}_{n,i}(y)| \stackrel{a.s.}{=} \mathcal{O}(n^{-1/2} \log n).$$

Next, for Thm. C, we have

$$\begin{aligned} (25) \quad & \limsup_{n \rightarrow \infty} \sup_{i \in [k]} \sup_{\delta_n \leq y \leq 1 - \delta_n} (y(1-y) \log \log n)^{-1/2} |u_{n,i}(y)| \\ &= \sup_{i \in [k]} \limsup_{n \rightarrow \infty} \sup_{\delta_n \leq y \leq 1 - \delta_n} (y(1-y) \log \log n)^{-1/2} |u_{n,i}(y)| \\ &\stackrel{(24)}{\leq} \sup_{i \in [k]} 4 = 4. \end{aligned}$$

For Thm. D, we claim that we have the same asymptotic behavior in our case (proven at the end of this section)

$$\begin{aligned} (26) \quad & \sup_{i \in [k]} \sup_{0 < y < 1} |f(F^{-1}(y))q_n(y) - u_n(y)| \\ &\stackrel{a.s.}{=} \begin{cases} \mathcal{O}(n^{-1/2} \log \log n) & \text{if } \gamma < 1 \\ \mathcal{O}(n^{-1/2} (\log \log n)^2) & \text{if } \gamma = 1 \\ \mathcal{O}(n^{-1/2} (\log \log n)^\gamma (\log n)^{(1+\varepsilon)(\gamma-1)}) & \text{if } \gamma > 1 \end{cases} \end{aligned}$$

Putting these pieces together, we get

$$\begin{aligned} & \sup_{i \in [k]} \sup_{0 < y < 1} |f_i(F_i^{-1}(y))\hat{q}_{n,i}(y) - \mathbb{B}_{n,i}(y)| \\ &\stackrel{(b)}{\leq} \sup_{i \in [k]} \sup_{0 < y < 1} |f_i(F_i^{-1}(y))\hat{q}_{n,i}(y) - u_{n,i}(y)| + |u_{n,i}(y) - \mathbb{B}_{n,i}(y)| \\ &\stackrel{(c)}{=} \mathcal{O}(n^{-1/2} \log n + n^{-1/2} (\log \log n)^2) \\ &= \mathcal{O}(n^{-1/2} \log n) \end{aligned}$$

where (b) follows from the triangle inequality and (c) follows because $\gamma < 2$ for each measure and we can set $\varepsilon < 1/(\gamma - 1) - 1$ if $1 < \gamma < 2$ in (26).

We can now finish the main proof. From Assum. 3, there exists a positive constant C that lower bounds each density function. Thus, for n large enough (which we have shown exists for any admissible value of k), we have for some universal constant c

$$\begin{aligned} (27) \quad & \sup_{j \in [k]} \sup_{0 < y < 1} \left| f_j(F_j^{-1}(y))\hat{q}_{n,j}(y) - \mathbb{B}_{n,j}(y) \right| \stackrel{a.s.}{\leq} c(n^{-1/2} \log n + kn^{-1/2} (\log \log n)^2) \\ & \sup_{j \in [k]} \sup_{0 < y < 1} \left| \hat{q}_{n,j}(y) - \frac{\mathbb{B}_{n,j}(y)}{f_j(F_j^{-1}(y))} \right| \stackrel{a.s.}{\leq} \frac{c}{C}(n^{-1/2} \log n + kn^{-1/2} (\log \log n)^2) \end{aligned}$$

Then, for any $y \in (0, 1)$, almost surely,

$$\left| \frac{1}{k} \sum_{j=1}^k \left(\hat{q}_{\nu_j, n}(y) - \frac{\mathbb{B}_{n,j}(y)}{f_j(F_j^{-1}(y))} \right) \right| \stackrel{(c)}{\leq} \frac{1}{k} \sum_{j=1}^k \left| \hat{q}_{\nu_j, n}(y) - \frac{\mathbb{B}_{n,j}(y)}{f_j(F_j^{-1}(y))} \right|$$

$$\stackrel{(27)}{\leq} \frac{c}{C} n^{-1/2} \log n$$

where (c) follows the triangle inequality. Next, since this holds for all y , we can take the $L^2(0, 1)$ of both sides to get

$$\frac{1}{n} \left\| \frac{1}{k} \sum_{j=1}^k \left(\hat{q}_{\nu_j, n}(y) - \frac{\mathbb{B}_{n,j}(y)}{f_j(F_j^{-1}(y))} \right) \right\|_{L^2(0,1)}^2 \leq \frac{c}{n^2 C} \log^2 n = \mathcal{O}\left(\frac{\log^2 n}{n^2}\right).$$

Proof of claim (26). We will only repeat the parts of the proof that differ in our case. Let $y \in ((l-1)/n, l/n]$ and ξ be between y and $U_{l:n} = y + \sqrt{n}u_n(y)$. Then, we have from [19, Eq. 3.8]

$$\sup_{i \in [k]} |f_i(F_i^{-1}(y)) \hat{q}_{n,i}(y) - u_{n,i}(y)| \leq \sup_{i \in [k]} \frac{1}{2} n^{-1/2} u_{n,i}^2(y) f_i(F_i^{-1}(y)) \frac{|f'_i(F_i^{-1}(\xi))|}{f_i^3(F_i^{-1}(\xi))}.$$

Next, from (25) and since each term is nonnegative, we have for large enough n

$$\sup_{i \in [k]} |f_i(F_i^{-1}(y)) \hat{q}_{n,i}(y) - u_{n,i}(y)|$$

$$\leq 8n^{-1/2} (\log \log n) y (1-y) \sup_{i \in [k]} f_i(F_i^{-1}(y)) \frac{|f'_i(F_i^{-1}(\xi))|}{f_i^3(F_i^{-1}(\xi))}.$$

From the proof of [19, Thm. 3], we have

$$\sup_{i \in [k]} |f_i(F_i^{-1}(y)) \hat{q}_{n,i}(y) - u_{n,i}(y)| \leq 8\gamma 5 \cdot 10^\gamma n^{-1/2} (\log \log n).$$

Next, from [19, Eq. 3.10], we have

$$\sup_{i \in [k]} \sup_{0 \leq y \leq \delta_n} |u_n(y)| \stackrel{a.s.}{\leq} 45 n^{-1/2} \log \log n.$$

From [19, Eq. 3.13], if $U_{l:n} \geq y$, then

$$\sup_{i \in [k]} |f_i(F_i^{-1}(y)) q_{n,i}(y)| \leq u_n(y).$$

If $U_{k:n} < y$, then [19, Eq. 3.14] establishes

$$\sup_{i \in [k]} |f_i(F_i^{-1}(y)) q_{n,i}(y)| \leq \begin{cases} \frac{2^\gamma}{1-\gamma} n^{1/2} y & \text{if } \gamma < 1 \\ \frac{2^\gamma}{\gamma-1} n^{1/2} y^\gamma U_{l:n}^{-(\gamma-1)} & \text{if } \gamma > 1 \\ 2n^{1/2} y \log(y/U_{l:n}) & \text{if } \gamma = 1 \end{cases}$$

Next, from the end of proof of [19, Thm. 3], we have our result.

A.1.2. Proof of Lem. 2: Norm of average of Brownian bridges. We need to show that Prop. 1 holds with constants that do not depend on k . We have

$$\frac{1}{n} \left\| \frac{1}{k} \sum_{j=1}^k w_j \cdot \mathbb{B}_j \right\|_{L^2(0,1)}^2 = \frac{1}{nk} \left\| \underbrace{\frac{1}{\sqrt{k}} \sum_{j=1}^k w_j \cdot \mathbb{B}_j}_{\mathbb{G}_k} \right\|_{L^2(0,1)}^2.$$

Clearly, \mathbb{G}_k is a Gaussian process with $\mathbb{E}[\mathbb{G}_k(t)] = 0$ and $\mathbb{G}_k(0) = \mathbb{G}_k(1) = 0$. We also know that it has continuous sample paths and is thus bounded. However, we wish to show that it is uniformly bounded over all values of k . For $s, t \in [0, 1]$, we have

$$\begin{aligned} \text{Cov}(\mathbb{G}_k(s), \mathbb{G}_k(t)) &= \frac{1}{k} \text{Cov}\left(\sum_{j=1}^k w_j(s) \mathbb{B}_j(s), \sum_{j=1}^k w_j(t) \mathbb{B}_j(t)\right) \\ &\stackrel{(a)}{=} \frac{1}{k} \sum_{j=1}^k \text{Cov}(w_j(s) \mathbb{B}_j(s), w_j(t) \mathbb{B}_j(t)) \\ &= \frac{1}{k} \sum_{j=1}^k w_j(s) w_j(t) (\min(s, t) - st) \end{aligned}$$

where (a) follows from the independence on the Brownian bridges. Next, we have for all $j \in [k]$ and $t \in [0, 1]$, $w_j(t) < C'$ for some universal C' . Thus,

(28)

$$\text{Var}(\mathbb{G}_k(t)) = \text{Cov}(\mathbb{G}_k(t), \mathbb{G}_k(t)) = \frac{1}{k} \sum_{j=1}^k (w_j(t))^2 (t - t^2) \leq (t - t^2) C'^2 \leq (0.5) C'^2.$$

Let $\sigma_{\mathbb{G}_k}^2 \triangleq \sup_{t \in [0, 1]} \mathbb{E}[(\mathbb{G}_k(t))^2]$. Since we have that almost surely, the paths of \mathbb{G}_k are bounded, then by the Borell–TIS inequality [2, Thm. 2.1.1], we have that for $u > 0$,

$$\mathbb{P}\left(\sup_{t \in [0, 1]} \mathbb{G}_k(t) - \mathbb{E}\left[\sup_{t \in [0, 1]} \mathbb{G}_k(t)\right] > u\right) \leq \exp(-u^2 / (2\sigma_{\mathbb{G}_k}^2)) \stackrel{(28)}{\leq} \exp(-u^2 / C'^2).$$

Rewriting, we get

$$\mathbb{P}\left(\sup_{t \in [0, 1]} \mathbb{G}_k(t) \leq u + \mathbb{E}\left[\sup_{t \in [0, 1]} \mathbb{G}_k(t)\right]\right) \geq 1 - \exp(-u^2 / C'^2).$$

The final step is to provide a uniform upper bound on $\mathbb{E}[\sup_{t \in [0, 1]} \mathbb{G}_k(t)]$. From Dudley's theorem [2, Thm. 1.3.13], there exists a universal constant K such that

$$(29) \quad \mathbb{E}\left[\sup_{t \in [0, 1]} \mathbb{G}_k(t)\right] \leq K \int_0^{\text{diam}([0, 1])/2} \sqrt{\log(\mathcal{N}([0, 1], d, \varepsilon))} d\varepsilon$$

where $d(s, t) = (\mathbb{E}[(\mathbb{G}_k(s) - \mathbb{G}_k(t))^2])^{1/2}$, $\text{diam}([0, 1])$ is the maximum distance under d between two points in $[0, 1]$, and $\mathcal{N}([0, 1], d, \varepsilon)$ is the smallest number of balls of length ε that cover $[0, 1]$ under d . Next, we claim that there is a constant $\tilde{C} > 0$ such that

$$(30) \quad (d(s, t))^2 \leq \tilde{C} |s - t|.$$

We prove this claim in App. A.2. So, we can provide the following upper bounds:

$$\text{diam}([0, 1]) = \max_{s, t \in [0, 1]} d(s, t) \leq \sqrt{\tilde{C}}, \quad \text{and}$$

$$\mathcal{N}([0, 1], d, \varepsilon) \leq \mathcal{N}([0, 1], |\cdot|, \varepsilon^2 / \tilde{C}) \stackrel{(a)}{\leq} \begin{cases} \frac{3\tilde{C}}{\varepsilon^2} & \text{if } \varepsilon \leq \sqrt{\tilde{C}} \\ 1 & \text{if } \varepsilon > \sqrt{\tilde{C}} \end{cases}$$

where (a) follows from [47, Eq. 4.10]. Plugging this into (29), we get

$$\mathbb{E} \left[\sup_{t \in [0,1]} \mathbb{G}_k(t) \right] \leq K \int_0^{\sqrt{\tilde{C}}/2} \sqrt{\log \left(\frac{3\tilde{C}}{\varepsilon^2} \right)} d\varepsilon \triangleq \tilde{K} < \infty.$$

Going back to the probability term, we get

$$\mathbb{P} \left(\sup_{t \in [0,1]} \mathbb{G}_k(t) \leq u + \tilde{K} \right) \geq 1 - \exp(-u^2/C'^2).$$

Thus, we have that $\sup_{t \in [0,1]} \mathbb{G}_k(t) = \mathcal{O}_p(1)$ with constants that do not depend on k or the functions w_j . Thus, we have that

$$\|\mathbb{G}_k\|_{L^2(0,1)}^2 \leq \left\| \sup_{t \in [0,1]} \mathbb{G}_k(t) \right\|_{L^2(0,1)}^2 = \left(\sup_{t \in [0,1]} \mathbb{G}_k(t) \right)^2 = \mathcal{O}_p(1).$$

A.2. Proof of claim (30). First, let $t \geq s$. Since \mathbb{G}_k has mean 0 at any time,

$$\begin{aligned} (d(t, s))^2 &= \mathbb{E}[(\mathbb{G}_k(t) - \mathbb{G}_k(s))^2] \\ &= \text{Var}(\mathbb{G}_k(t) - \mathbb{G}_k(s)) \\ &= \text{Var}(\mathbb{G}_k(t)) + \text{Var}(\mathbb{G}_k(s)) - 2\text{Cov}(\mathbb{G}_k(t), \mathbb{G}_k(s)) \\ &= \frac{1}{k} \sum_{j=1}^k [w_j(t)^2(t - t^2) + w_j(s)^2(s - s^2) - 2w_j(t)w_j(s)(s - st)] \end{aligned}$$

Now, we just consider one summand since the bound will apply for all summands:

$$\begin{aligned} &w_j^2(t)(t - t^2) + w_j^2(s)(s - s^2) - 2w_j(t)w_j(s)(s - st) \\ &= w_j^2(t)t - w_j^2(t)t^2 + w_j^2(s)s - w_j^2(s)s^2 - 2w_j(t)w_j(s)s + 2w_j(t)w_j(s)st \\ &= w_j^2(s)s - 2w_j(t)w_j(s)s + w_j^2(t)s - w_j^2(t)s + w_j^2(t)t \\ &\quad - w_j^2(t)t^2 - w_j^2(s)s^2 + 2w_j(t)w_j(s)st \\ &= w_j^2(s)s - 2w_j(t)w_j(s)s + w_j^2(t)s - w_j^2(t)s + w_j^2(t)t - (w_j(t)t - w_j(s)s)^2 \\ &\leq w_j^2(s)s - 2w_j(t)w_j(s)s + w_j^2(t)s - w_j^2(t)s + w_j^2(t)t \\ &= s(w_j(t) - w_j(s))^2 + w_j^2(t)(t - s) \\ &\leq (w_j(t) - w_j(s))^2 + w_j^2(t)(t - s) \\ &\stackrel{(a)}{\leq} L^2(t - s)^2 + w_j^2(t)(t - s) \\ &\stackrel{(b)}{\leq} \tilde{C}(t - s) \end{aligned}$$

where (a) follows from the w_j functions being L -Lipschitz, and (b) follows from the fact that $t, s \in [0, 1]$ and there is a multiplicative constant that makes $(t - s)$ dominate $(t - s)^2$ within $[0, 1]$.

A.3. Proof of claim (16): Asymptotic bias bound. We start by breaking up the bias into its components:

$$\begin{aligned}
W_2(\bar{\mu}_{ij}, \mu_{ij}) &\stackrel{(3)}{=} \left\| F_{\bar{\mu}_{ij}}^{-1} - F_{\mu_{ij}}^{-1} \right\|_{L^2(0,1)} \stackrel{(21)}{=} \left\| \frac{1}{|\mathcal{N}_{i,\eta}|} \sum_{k \in \mathcal{N}_{i,\eta}} (F_{\mu_{kj}}^{-1} - F_{\mu_{ij}}^{-1}) \right\|_{L^2(0,1)} \\
&= \frac{1}{|\mathcal{N}_{i,\eta}|} \left\| \sum_{k \in \mathcal{N}_{i,\eta}} (F_{\mu_{kj}}^{-1} - F_{\mu_{ij}}^{-1}) \right\|_{L^2(0,1)} \\
&\stackrel{(a)}{\leq} \frac{1}{|\mathcal{N}_{i,\eta}|} \sum_{k \in \mathcal{N}_{i,\eta}} \left\| F_{\mu_{kj}}^{-1} - F_{\mu_{ij}}^{-1} \right\|_{L^2(0,1)} \\
&\leq \frac{|\mathcal{N}_{i,\eta}|}{|\mathcal{N}_{i,\eta}|} \max_{k \in \mathcal{N}_{i,\eta}} \left\| F_{\mu_{kj}}^{-1} - F_{\mu_{ij}}^{-1} \right\|_{L^2(0,1)} \\
&\stackrel{(3)}{=} \max_{k \in \mathcal{N}_{i,\eta}} W_2(\mu_{kj}, \mu_{ij}).
\end{aligned}$$

where (a) follows from Minkowski's inequality [30, Thm. 198]. By nonnegativity and squaring, we have

$$W_2^2(\bar{\mu}_{ij}, \mu_{ij}) \leq \max_{k \in \mathcal{N}_{i,\eta}} W_2^2(\mu_{kj}, \mu_{ij}).$$

Next, we claim that

$$(31) \quad \mathbb{E} \left[\rho_{iu} \mid x_{\text{row}}^{(i)}, x_{\text{row}}^{(u)} \right] = \mathbb{E} \left[W_2^2(Y_{ij}, Y_{uj}) \mid x_{\text{row}}^{(i)}, x_{\text{row}}^{(u)} \right]$$

which we prove at the end of this section. Since the latent spaces are bounded and the latent function f is Lipschitz, then the space of distributions is also bounded in Wasserstein distance. Since the space is bounded in Wasserstein distance and since each distribution has finite support, then there exists a universal constant y_{\max} such that $W_2^2(Y_{ij}, Y_{uj}) \leq y_{\max}$. Thus, we have⁴

$$\|W_2^2(Y_{ij}, Y_{uj})\|_{\psi_2} \leq \frac{y_{\max}}{\sqrt{\ln(2)}} = K.$$

So, by the Hoeffding Inequality (Theorem 2.6.3 in [47]), we have that for any fixed row u ,

$$\mathbb{P} \left(|\rho_{ik} - \mathbb{E}[W_2^2(Y_{ij}, Y_{uj})]| \geq t \mid \mathcal{C}_{iu}, x_{\text{row}}^{(i)}, x_{\text{row}}^{(u)} \right) \leq 2 \exp \left(-c \frac{t^2}{K^2} |\mathcal{C}_{iu}| \right).$$

So, by total probability, we have

$$\begin{aligned}
&\mathbb{P} \left(|\rho_{iu} - \mathbb{E}[W_2^2(Y_{ij}, Y_{uj})]| \geq t \mid x_{\text{row}}^{(i)}, x_{\text{row}}^{(u)} \right) \\
&\leq \mathbb{P} \left(|\rho_{iu} - \mathbb{E}[W_2^2(Y_{ij}, Y_{uj})]| \geq t \mid |\mathcal{C}_{ik}| \geq \frac{1}{2} M p^2, x_{\text{row}}^{(i)}, x_{\text{row}}^{(u)} \right) \\
&\quad + \mathbb{P} \left(|\mathcal{C}_{ik}| \leq \frac{1}{2} M p^2, x_{\text{row}}^{(i)}, x_{\text{row}}^{(u)} \right) \\
&\leq 2 \exp \left(-c \frac{t^2}{2K^2} M p^2 \right) + \exp \left(-\frac{1}{8} M p^2 \right).
\end{aligned}$$

⁴The Orlicz ψ_2 norm is defined as $\|X\|_{\psi_2} = \inf_{t>0} \mathbb{E} \left[\exp(|X|^2/t^2) \leq 2 \right]$.

Taking a union bound, we can remove the conditioning to get

$$(32) \quad \mathbb{P}\left(\max_{k \neq i} |\rho_{ik} - \mathbb{E}[W_2^2(Y_{ij}, Y_{kj})]| \leq t\right) \\ \geq 1 - 2N \exp\left(-c \frac{t^2}{2K^2} Mp^2\right) - N \exp\left(-\frac{1}{8} Mp^2\right).$$

Denote the event above as \mathcal{E} . Since the latent metric spaces \mathcal{H}_{row} and \mathcal{H}_{col} are bounded and since the latent function f is L -Lipschitz with respect to its row argument, then there exists a constant $c_f \geq 0$ where

$$(33) \quad W_2^2(\mu_{kj}, \mu_{ij}) \leq c_f \mathbb{E}_{x \sim \mathcal{H}_{\text{col}}} \left[W_2^2(f(x_{\text{row}}^{(k)}, x), f(x_{\text{row}}, x)) \right]$$

where $x \sim \mathcal{H}_{\text{col}}$ means that x is drawn from the distribution over the column latent space. Next, we have from [40, Lem. 3] that for any distributions μ and ν with respective empirical distributions $\hat{\mu}$ and $\hat{\nu}$ derived from n samples each,

$$(34) \quad \mathbb{E}[W_2^2(\hat{\mu}, \hat{\nu})] \geq W_2^2(\mu, \nu)$$

where the expectation is taken over the randomness in the sampling. So, we have that on event \mathcal{E} ,

$$\begin{aligned} \max_{k \in \mathcal{N}_{i,\eta}} W_2^2(\mu_{kj}, \mu_{ij}) &\stackrel{(33)}{\leq} \max_{k \in \mathcal{N}_{i,\eta}} c_f \mathbb{E}_{x \sim \mathcal{H}_{\text{col}}} \left[W_2^2(f(x_{\text{row}}^{(k)}, x), f(x_{\text{row}}, x)) \right] \\ &\stackrel{(34)}{\leq} \max_{k \in \mathcal{N}_{i,\eta}} c_f \mathbb{E}_{\mathcal{H}_{\text{col}}} [\mathbb{E}[W_2^2(Y_{kj}, Y_{ij})]] \\ &\stackrel{(32)}{\leq} \max_{k \in \mathcal{N}_{i,\eta}} c_f (\rho_{ik} + t) \\ &\leq c_f (\eta + t). \end{aligned}$$

Putting this together, we have

$$\begin{aligned} \mathbb{P}(W_2^2(\bar{\mu}_{ij}, \mu_{ij}) \leq c_f (\eta + t) \mid |\mathcal{N}_{i,\eta}| \geq 1) \\ \geq 1 - 2N \exp\left(-c \frac{t^2}{2K^2} Mp^2\right) - N \exp\left(-\frac{1}{8} Mp^2\right). \end{aligned}$$

Finally, it can be easily verified that by setting

$$t = K \sqrt{\frac{2}{cMp^2} \log\left(\frac{2N}{\delta}\right)}$$

we get

$$\begin{aligned} \mathbb{P}\left(2W_2^2(\bar{\mu}_{ij}, \mu_{ij}) \leq 2c_f \left(\eta + K \sqrt{\frac{2}{cMp^2} \log\left(\frac{2N}{\delta}\right)}\right) \mid |\mathcal{N}_{i,\eta}| \geq 1\right) \\ \geq 1 - \delta - N \exp\left(-\frac{1}{8} Mp^2\right). \end{aligned}$$

Now, we will prove that this quantity is bounded in probability as $M \rightarrow \infty$. Let $0 < \epsilon < 1$ be arbitrary. Then, there exists a δ and large enough M_0 such that for all $M \geq M_0$, $\epsilon \leq$

$\delta + N \exp(-\frac{1}{8}Mp^2)$. Plugging this into the inequality above, we get that

$$\begin{aligned} & \mathbb{P}\left(W_2^2(\bar{\mu}_{ij}, \mu_{ij}) \leq c_f \left(\eta + \sqrt{\frac{2K^2}{cMp^2} \log\left(\frac{2N}{\delta}\right)} \right) \mid |\mathcal{N}_{i,\eta}| \geq 1\right) \\ & \geq 1 - \delta - N \exp\left(-\frac{1}{8}Mp^2\right) \\ & \geq 1 - \epsilon. \end{aligned}$$

Rewriting the left-hand side, we get

$$\begin{aligned} W_2^2(\bar{\mu}_{ij}, \mu_{ij}) & \leq c_f \left(\eta + K \sqrt{\frac{2}{cMp^2} \log\left(\frac{2N}{\delta}\right)} \right) \\ W_2^2(\bar{\mu}_{ij}, \mu_{ij}) - c_f \eta & \leq c_f K \sqrt{\frac{2}{cMp^2} \log\left(\frac{2N}{\delta}\right)} \\ \frac{W_2^2(\bar{\mu}_{ij}, \mu_{ij}) - c_f \eta}{\sqrt{2(cMp^2)^{-1}}} & \leq c_f K \sqrt{\log(2N/\delta)}. \end{aligned}$$

Thus, since we keep N fixed, then by the definition of bounded in probability we have

$$W_2^2(\bar{\mu}_{ij}, \mu_{ij}) = \mathcal{O}_p(\eta + (Mp^2)^{-1/2}) \quad \text{as } M \rightarrow \infty.$$

A.4. Proof of claim (31). Recall the definition of ρ_{iu} from (6):

$$\rho_{iu} \triangleq \begin{cases} \frac{1}{|\mathcal{C}_{iu}|} \sum_{j \in \mathcal{C}_{iu}} W_2^2(Y_{ij}, Y_{uj}) & \text{if } |\mathcal{C}_{iu}| \geq 1 \\ \infty & \text{if } |\mathcal{C}_{iu}| = 0. \end{cases}$$

Let \mathbb{S} denote the randomness from sampling n points from each distribution. Next, we only need to consider the case of $|\mathcal{C}_{iu}| \geq 1$ because we give a high-probability bound on this quantity being large. Under this, we have

$$\begin{aligned} \mathbb{E}[\rho_{iu} \mid \mathcal{C}_{iu}, x_{\text{row}}^{(i)}, x_{\text{row}}^{(u)}] & = \mathbb{E}\left[\frac{1}{|\mathcal{C}_{iu}|} \sum_{j \in \mathcal{C}_{iu}} W_2^2(Y_{ij}, Y_{uj}) \mid \mathcal{C}_{iu}, x_{\text{row}}^{(i)}, x_{\text{row}}^{(u)}\right] \\ & = \frac{1}{|\mathcal{C}_{iu}|} \sum_{j \in \mathcal{C}_{iu}} \mathbb{E}[W_2^2(Y_{ij}, Y_{uj}) \mid \mathcal{C}_{iu}, x_{\text{row}}^{(i)}, x_{\text{row}}^{(u)}] \\ & = \frac{1}{|\mathcal{C}_{iu}|} \sum_{j \in \mathcal{C}_{iu}} \mathbb{E}[W_2^2(Y_{ij}, Y_{uj}) \mid x_{\text{row}}^{(i)}, x_{\text{row}}^{(u)}] \end{aligned}$$

where the last line follows from the independence of the missingness from the distributions. This expectation is taken over two sources of randomness: the distribution over \mathcal{H}_{col} and the distribution over the sampling from each distribution, \mathbb{S} . Next, since each sample is drawn i.i.d. and since each column vector is also drawn i.i.d then we have that $\mathbb{E}[W_2^2(Y_{ij}, Y_{uj}) \mid x_{\text{row}}^{(i)}, x_{\text{row}}^{(u)}]$ is constant across column latent vectors. Thus, we have that

$$\mathbb{E}[\rho_{iu} \mid \mathcal{C}_{iu}, x_{\text{row}}^{(i)}, x_{\text{row}}^{(u)}] = \mathbb{E}[W_2^2(Y_{ij}, Y_{uj}) \mid x_{\text{row}}^{(i)}, x_{\text{row}}^{(u)}].$$

Since this holds for all \mathcal{C}_{iu} , we can remove the conditioning to get our claim:

$$\mathbb{E}[\rho_{iu} \mid x_{\text{row}}^{(i)}, x_{\text{row}}^{(u)}] = \mathbb{E}[W_2^2(Y_{ij}, Y_{uj}) \mid x_{\text{row}}^{(i)}, x_{\text{row}}^{(u)}].$$

APPENDIX B: PROOF OF THM. 2 - ASYMPTOTIC DISTRIBUTION OF ESTIMATE

Let $t \in (0, 1)$. First, we can do a similar bias-variance decomposition as in (14):

$$F_{\hat{\mu}_{ij}}^{-1}(t) - F_{\mu_{ij}}^{-1}(t) = F_{\hat{\mu}_{ij}}^{-1}(t) - F_{\bar{\mu}_{ij}}^{-1}(t) + F_{\bar{\mu}_{ij}}^{-1}(t) - F_{\mu_{ij}}^{-1}(t).$$

We claim that

$$(35) \quad \frac{\sqrt{n_{j,M}|\mathcal{N}_{i,\eta_M}|}}{\sigma_{\mathcal{N}_{i,\eta_M}}(t)} (F_{\hat{\mu}_{ij}}^{-1}(t) - F_{\bar{\mu}_{ij}}^{-1}(t)) \xrightarrow{d} \mathcal{N}(0, 1)$$

and

$$(36) \quad \frac{\sqrt{n_{j,M}|\mathcal{N}_{i,\eta_M}|}}{\sigma_{\mathcal{N}_{i,\eta_M}}(t)} (F_{\bar{\mu}_{ij}}^{-1}(t) - F_{\mu_{ij}}^{-1}(t)) = o_p(1).$$

We use the following fact to prove both claims for random variables X_m :

$$\text{if } X_m = \mathcal{O}_p(a_m) \quad \text{and} \quad \lim_{m \rightarrow \infty} a_m = 0 \quad \text{then} \quad X_m = o_p(1).$$

Putting together claims (35) and (36), we have

$$\frac{\sqrt{n_{j,M}|\mathcal{N}_{i,\eta_M}|}}{\sigma_{\mathcal{N}_{i,\eta_M}}(t)} (F_{\hat{\mu}_{ij}}^{-1}(t) - F_{\mu_{ij}}^{-1}(t)) \xrightarrow{d} \mathcal{N}(0, 1).$$

B.1. Proof of claim (35). First, define $\hat{q}_{uj}(t) \triangleq \sqrt{n_{j,M}}(F_{Y_{uj}}^{-1}(t) - F_{\mu_{uj}}^{-1}(t))$. Recall from the proof of Prop. 1 that we have that for each distribution μ_{uj} for $u \in \mathcal{N}_{i,\eta_M}$ and its respective approximation by a sequence of standard Brownian bridges, $(\mathbb{B}_{u,l})_{l=1}^{n_{j,M}}$,

$$\sup_{t \in (0,1)} \left| \hat{q}_{uj}(t) - \frac{\mathbb{B}_{u,n_{j,M}}(t)}{f_{\mu_{uj}}(F_{\mu_{uj}}^{-1}(t))} \right| \stackrel{a.s.}{=} \mathcal{O}\left(\frac{\log n_{j,M}}{\sqrt{n_{j,M}}}\right).$$

Next, we have

$$\begin{aligned} \sqrt{n_{j,M}|\mathcal{N}_{i,\eta_M}|} (F_{\hat{\mu}_{ij}}^{-1}(t) - F_{\bar{\mu}_{ij}}^{-1}(t)) &\stackrel{(8)}{=} \sqrt{n_{j,M}|\mathcal{N}_{i,\eta_M}|} \left(\frac{1}{|\mathcal{N}_{i,\eta_M}|} \sum_{u \in \mathcal{N}_{i,\eta_M}} F_{Y_{uj}}^{-1}(t) - F_{\mu_{uj}}^{-1}(t) \right) \\ &= \frac{1}{\sqrt{|\mathcal{N}_{i,\eta_M}|}} \sum_{u \in \mathcal{N}_{i,\eta_M}} \hat{q}_{uj}(t) \end{aligned}$$

Now, we will proceed similar to the proof of Prop. 1 by adding and subtracting the Brownian bridge approximation:

$$\begin{aligned} &\frac{1}{\sqrt{|\mathcal{N}_{i,\eta_M}|}} \sum_{u \in \mathcal{N}_{i,\eta_M}} \hat{q}_{uj}(t) \\ &= \frac{1}{\sqrt{|\mathcal{N}_{i,\eta_M}|}} \sum_{u \in \mathcal{N}_{i,\eta_M}} \left(\hat{q}_{uj}(t) - \frac{\mathbb{B}_{u,n_{j,M}}(t)}{f_{\mu_{uj}}(F_{\mu_{uj}}^{-1}(t))} + \frac{\mathbb{B}_{u,n_{j,M}}(t)}{f_{\mu_{uj}}(F_{\mu_{uj}}^{-1}(t))} \right) \\ &= \frac{1}{\sqrt{|\mathcal{N}_{i,\eta_M}|}} \sum_{u \in \mathcal{N}_{i,\eta_M}} \left(\hat{q}_{uj}(t) - \frac{\mathbb{B}_{u,n_{j,M}}(t)}{f_{\mu_{uj}}(F_{\mu_{uj}}^{-1}(t))} \right) + \frac{1}{\sqrt{|\mathcal{N}_{i,\eta_M}|}} \sum_{u \in \mathcal{N}_{i,\eta_M}} \frac{\mathbb{B}_{u,n_{j,M}}(t)}{f_{\mu_{uj}}(F_{\mu_{uj}}^{-1}(t))} \end{aligned}$$

Analyzing the first sum, we have from the following bound from applying Prop. 1 just like in the proof of Lem. 1:

$$\begin{aligned}
& \frac{1}{\sqrt{|\mathcal{N}_{i,\eta_M}|}} \sum_{u \in \mathcal{N}_{i,\eta_M}} \left(\hat{q}_{uj}(t) - \frac{\mathbb{B}_{u,n_{j,M}}(t)}{f_{\mu_{uj}}(F_{\mu_{uj}}^{-1}(t))} \right) \\
& \leq \left| \frac{1}{\sqrt{|\mathcal{N}_{i,\eta_M}|}} \sum_{u \in \mathcal{N}_{i,\eta_M}} \left(\hat{q}_{uj}(t) - \frac{\mathbb{B}_{u,n_{j,M}}(t)}{f_{\mu_{uj}}(F_{\mu_{uj}}^{-1}(t))} \right) \right| \\
& \stackrel{(a)}{\leq} \frac{1}{\sqrt{|\mathcal{N}_{i,\eta_M}|}} \sum_{u \in \mathcal{N}_{i,\eta_M}} \left| \hat{q}_{uj}(t) - \frac{\mathbb{B}_{u,n_{j,M}}(t)}{f_{\mu_{uj}}(F_{\mu_{uj}}^{-1}(t))} \right| \\
& \stackrel{(22)}{=} \mathcal{O} \left(\sqrt{|\mathcal{N}_{i,\eta_M}|} \frac{\log n_{j,M}}{\sqrt{n}} \right) \\
& \stackrel{(12)}{=} o_p(1)
\end{aligned}$$

where (a) follows from the triangle inequality. Analyzing the second sum, we have

$$\frac{1}{\sqrt{|\mathcal{N}_{i,\eta_M}|}} \sum_{u \in \mathcal{N}_{i,\eta_M}} \frac{\mathbb{B}_{u,n_{j,M}}(t)}{f_{\mu_{uj}}(F_{\mu_{uj}}^{-1}(t))} \stackrel{d}{=} \frac{1}{\sqrt{|\mathcal{N}_{i,\eta_M}|}} \sum_{u \in \mathcal{N}_{i,\eta_M}} \frac{X_u}{f_{\mu_{uj}}(F_{\mu_{uj}}^{-1}(t))}$$

where $\{X_u\}_{u \in \mathcal{N}_{i,\eta_M}}$ are i.i.d. $\mathcal{N}(0, t - t^2)$ random variables because $\mathbb{B}_{u,n_{j,M}}(t) \sim \mathcal{N}(0, t - t^2)$ from the definition of a standard Brownian bridge [42, Prop. 8.1.1]. Next, the sum of independent mean-zero Gaussian random variables is Gaussian with a variance equal to the sum of summand's variances and mean-zero. Thus, we have

$$\begin{aligned}
& \frac{1}{\sqrt{|\mathcal{N}_{i,\eta_M}|}} \sum_{u \in \mathcal{N}_{i,\eta_M}} \frac{X_u}{f_{\mu_{uj}}(F_{\mu_{uj}}^{-1}(t))} \sim \mathcal{N} \left(0, \frac{1}{|\mathcal{N}_{i,\eta_M}|} \sum_{u \in \mathcal{N}_{i,\eta_M}} \frac{t - t^2}{f_{\mu_{uj}}^2(F_{\mu_{uj}}^{-1}(t))} \right) \\
& \stackrel{(11)}{=} \mathcal{N}(0, \sigma_{\mathcal{N}_{i,\eta}}^2(t))
\end{aligned}$$

Thus, we have

$$\frac{1}{\sigma_{\mathcal{N}_{i,\eta}}(t) \sqrt{|\mathcal{N}_{i,\eta_M}|}} \sum_{u \in \mathcal{N}_{i,\eta_M}} \frac{\mathbb{B}_{u,n_{j,M}}(t)}{f_{\mu_{uj}}(F_{\mu_{uj}}^{-1}(t))} \sim \mathcal{N}(0, 1)$$

which completes the proof of claim (35).

B.2. Proof of claim (36). Here, we consider the sequence $\frac{\sqrt{n_{j,M}|\mathcal{N}_{i,\eta_M}|}}{\sigma_{\mathcal{N}_{i,\eta_M}}(t)} (F_{\mu_{ij}}^{-1}(t) - F_{\mu_{ij}}^{-1}(t))$. From the proof of Thm. 1, we have:

$$(37) \quad \|F_{\mu_{ij}}^{-1} - F_{\mu_{ij}}^{-1}\|_{L^2(0,1)} \stackrel{(3)}{=} W_2(\bar{\mu}_{ij}, \mu_{ij}) \stackrel{(16)}{=} \mathcal{O}_p \left(\left(\eta_M + \sqrt{\frac{\log(2N_n)}{M_n p^2}} \right)^{1/2} \right).$$

Now, let $a_M(t) = \frac{\sqrt{n_{j,M}|\mathcal{N}_{i,\eta_M}|}}{\sigma_{\mathcal{N}_{i,\eta_M}}(t)}$. Thus, we have

$$\begin{aligned}
& \|a_M(t)(F_{\mu_{ij}}^{-1} - F_{\mu_{ij}}^{-1})\|_{L^2(0,1)} = a_M(t) \|F_{\mu_{ij}}^{-1} - F_{\mu_{ij}}^{-1}\|_{L^2(0,1)} \\
& \stackrel{(37)}{=} \mathcal{O}_p \left(a_M(t) \left(\eta_M + \sqrt{\frac{\log(2N_M)}{M p^2}} \right)^{1/2} \right) \\
& \stackrel{(12)}{=} o_p(1)
\end{aligned}$$

Next, from Assum. 3, each distribution has an L -Lipschitz quantile function and is thus continuously differentiable, which makes it Lipschitz as well. So, there exists a universal Lipschitz constant for the quantile functions since the union of all quantile functions have bounded range (because the union of the distributions has bounded support). Thus, $\{F_{\mu_{ij}}^{-1}\}_{n=1}^\infty$ is equicontinuous [13, Examples 11.15] (For the definition of equicontinuous sets of functions see [13, Ch. 11]. Next, from [28, Lem. 3.2], we know that if a sequence of equicontinuous functions converges in $L^2(0, 1)$ then it also converges uniformly. So, we have that for any $t \in (0, 1)$, $a_M(t)(F_{\mu_{ij}}^{-1}(t) - F_{\mu_{ij}}^{-1}(t)) = o_p(1)$.

APPENDIX C: COROLLARIES

Let $\phi(x, r) = \mathbb{P}_{\tilde{x} \sim \mathcal{H}_{\text{row}}}(\mathbb{E}_{v \sim \mathcal{H}_{\text{col}}}[W_2^2(f(x, v), f(\tilde{x}, v))] \leq r)$. We require the following two lemmas to remove the conditioning. First, we have a bound on the probability of having no neighbors: Next, we have a high-probability lower bound on the number of neighbors (proven in App. C.2):

LEMMA 3 (Lower bound on number of neighbors). *Let n_{-j} be the number of samples in each matrix entry not in column j . Let there exist constants c_1 and K such that $\eta' \geq \frac{6c_1}{n_{-j}}$ and $\eta \geq \eta' + K\sqrt{\frac{4\log(N)}{cMp^2}}$. Let $\mathcal{N}_{i,\eta}$ be the nearest neighbors for row i . Then we have*

$$\mathbb{P}\left(|\mathcal{N}_{i,\eta}| \geq \frac{1}{2}N\tilde{p}_{i,\eta'} \mid x_{\text{row}}^{(i)}\right) \geq 1 - \exp\left(-\frac{N\tilde{p}_{i,\eta'}}{8}\right) \quad \text{where}$$

$$\tilde{p}_{i,\eta'} \triangleq \left(1 - \frac{1}{N^2} - \exp\left(-\frac{Mp^2}{8}\right)\right) \cdot p \cdot \phi\left(x_{\text{row}}^{(i)}, \frac{\eta'}{3} - \frac{6c_1}{n_{-j}}\right).$$

Next, we have a simplified lower bound for the previous lemma:

LEMMA 4 (Simplified lower bound on number of neighbors). *We provide a simplified lower bound on $\frac{1}{2}N\hat{p}_{i,\eta'}$, to give a lower bound on the number of neighbors. For N, M large enough, we have*

$$\frac{1}{2}N\hat{p}_{i,\eta'} \geq \frac{1}{4}Np \cdot \phi\left(x_{\text{row}}^{(i)}, \frac{\eta'}{3} - \frac{6c_1}{n_{-j}}\right).$$

Now, we are prepared to state and prove our corollary.

C.1. Latent factors drawn from uniform hypercube. Here, we provide a general corollary where the latent factors are drawn from a uniform hypercube. This case covers Cor. 1.

COROLLARY 3 (Uniform measure on hypercube). *Let $\mathcal{H}_{\text{row}} = [0, 1]^d$ for some $d \geq 1$. Let Assums. 1 to 3 hold. Let d_{row} and d_{col} be the Euclidean measure and μ_{row} be the uniform measure. Let N, M , and p be fixed. Let $n_{-j} = n_v$ for $v \neq j$. Conditioned on $\mathcal{E} = \{|\mathcal{N}_{i,\eta}| \geq \frac{1}{4}(Np)^{\frac{2}{d+2}}\}$, we have*

$$W_2^2(\hat{\mu}_{ij}, \mu_{ij}) = \tilde{O}_p\left(\frac{1}{n_j(Np)^{\frac{2}{d+2}}} + \frac{\log^2 n_j}{n_j^2} + \frac{1}{p\sqrt{M}} + \frac{1}{n_{-j}}\right) \quad \text{as } n_j, M \rightarrow \infty, \quad \text{and}$$

$$\mathbb{P}(\mathcal{E}) \geq 1 - 2\exp\left(-(Np)^{\frac{2}{d+2}}/16\right).$$

PROOF OF COR. 3. Similar to Corollary 2 in [35], we define $B(x, r) \triangleq \{x' \in \mathcal{H}_{\text{row}} : d_{\text{row}}(x, x') \leq r\}$ for $r > 0$. Then, we have if $d_{\text{row}}(x, x') \leq \frac{1}{L} \left(\frac{\eta'}{3} - \frac{6c_1}{n_{-j}} \right)$, then by Lipschitz-ness of f , we have $\mathbb{E}_{v \sim \mu_{\text{col}}} [W_2^2(f(x, v) - f(x', v))] \leq \frac{\eta'}{3} - \frac{6c_1}{n_{-j}}$. Thus, we have

$$\phi\left(x, \frac{\eta'}{3} - \frac{6c_1}{n_{-j}}\right) \geq \mu_{\text{row}}\left(B\left(x, \frac{1}{L} \left(\frac{\eta'}{3} - \frac{6c_1}{n_{-j}} \right)\right)\right) = \text{Vol}\left(B\left(x, \frac{1}{L} \left(\frac{\eta'}{3} - \frac{6c_1}{n_{-j}} \right)\right)\right).$$

There are positive universal constants α and β such that for any $d \geq 1$, $x \in [0, 1]^d$, $r > 0$

$$\text{Vol}(B(x, r)) \geq \min(1, \alpha \beta^d r^d).$$

Plugging this into the inequality above, we have

$$\phi\left(x, \frac{\eta'}{3} - \frac{6c_1}{n_{-j}}\right) \geq \min\left\{1, \alpha \beta^d \left(\frac{1}{L} \left(\frac{\eta'}{3} - \frac{6c_1}{n_{-j}} \right)\right)^d\right\}$$

Next, $\forall v \in \mathcal{H}_{\text{col}}, x, x' \in \mathcal{H}_{\text{row}}, W_2(f(x, v), f(x', v)) \leq L\sqrt{d}$. Let

$$\frac{\eta'}{3} = \frac{6c_1}{n_{-j}} + \alpha^{2/d} \beta^2 L^2 (Mp)^{-2/(d+2)}.$$

So, we have

$$Np \cdot \phi\left(x, \frac{\eta'}{3} - \frac{6c_1}{n_{-j}}\right) \geq Np \cdot \frac{\left(\alpha^{-2/d} \beta^{-2} L^2 (Np)^{-2/(d+2)}\right)^{d/2}}{\alpha \beta^d L^d} = (Np)^{\frac{2}{d+2}}.$$

Putting this into the bounds in Lems. 3 and 4, and letting η' be equal to its lower bound, we get our result. \square

C.2. Proof of Lem. 3: Lower bound on number of neighbors. Now, we place a high-probability lower bound on the number of neighbors in order to remove the conditioning on $\mathcal{N}_{i, \eta}$. Now, we must remove the conditioning on $|\mathcal{N}_{i, \eta}|$. We do this by finding a high-probability bound on a another set which can be more easily analyzed:

$$\Omega \triangleq \{u \in [N+1] \setminus \{i\} : A_{uj} = 1, \mathbb{E}_{\mathcal{H}_{\text{col}}} [\mathbb{E}[W_2^2(Y_{iv}, Y_{uv})]] \leq \eta'\}.$$

Next, consider the set

$$\tilde{\Omega} \triangleq \{u \in \Omega : \rho_{iu} - \mathbb{E}_{\mathcal{H}_{\text{col}}} [\mathbb{E}[W_2^2(Y_{iv}, Y_{uv})]] \leq \eta - \eta'\}.$$

Since for $u \in \Omega$, $\mathbb{E}_{\mathcal{H}_{\text{col}}} [\mathbb{E}[W_2^2(Y_{iv}, Y_{uv})]] \leq \eta'$, then $\tilde{\Omega} \subseteq \mathcal{N}_{i, \eta}$. Thus, if we can provide a lower bound on $|\tilde{\Omega}|$, then this provides an upper bound on $\frac{1}{|\mathcal{N}_{i, \eta}|}$.

Next, we claim (proven at the end of this section)

$$(38) \quad \mathbb{P}\left(u \in \Omega \mid x_{\text{row}}^{(i)}\right) \geq p \cdot \phi\left(x_{\text{row}}^{(i)}, \frac{\eta'}{3} - \frac{6c_1}{n_{-j}}\right) \quad \text{and}$$

$$\mathbb{P}\left(u \in \tilde{\Omega} \mid u \in \Omega\right) \geq 1 - \frac{1}{N^2} - \exp\left(-\frac{Mp^2}{8}\right).$$

Putting these together, we find that

$$\begin{aligned} \mathbb{P}\left(u \in \tilde{\Omega} \mid x_{\text{row}}^{(i)}\right) &= \mathbb{P}\left(u \in \tilde{\Omega} \mid u \in \Omega, x_{\text{row}}^{(i)}\right) \mathbb{P}\left(u \in \Omega \mid x_{\text{row}}^{(i)}\right) \\ &\geq \left(1 - \frac{1}{N^2} - \exp\left(-\frac{Mp^2}{8}\right)\right) \cdot p \cdot \phi\left(x_{\text{row}}^{(i)}, \frac{\eta'}{3} - \frac{6c_1}{n_{-j}}\right) \\ &\triangleq \tilde{p}_{i, \eta'}. \end{aligned}$$

So, by the Binomial Chernoff bound, we get

$$\mathbb{P}\left(|\tilde{\Omega}| \geq \frac{1}{2}N\tilde{p}_{i,\eta'} \mid x_{\text{row}}^{(i)}\right) \geq 1 - \exp\left(-\frac{N\tilde{p}_{i,\eta'}}{8}\right)$$

and since $\tilde{\Omega} \subseteq \mathcal{N}_{i,\eta}$, then we have our result.

C.3. Proof of claim (38). We have that a row u is in Ω and satisfies the above inequality with probability $p \cdot \psi(x_{\text{row}}^{(i)}, \eta')$ where

$$\psi(x_{\text{row}}^{(i)}, \eta') = \mathbb{P}\left(\mathbb{E}[W_2^2(Y_{ij}, Y_{uj})] \leq \eta' \mid x_{\text{row}}^{(i)}\right).$$

By the Binomial Chernoff Bound and conditioning on the i -th latent row vector, we have

$$\begin{aligned} \mathbb{P}\left(|\Omega| = 0 \mid x_{\text{row}}^{(i)}\right) &\leq \mathbb{P}\left(|\Omega| \leq \frac{1}{2}Np \cdot \psi(x_{\text{row}}^{(i)}, \eta')\right) \\ &\leq \exp\left(-\frac{Np}{8}\psi(x_{\text{row}}^{(i)}, \eta')\right). \end{aligned}$$

Next, there exists a universal constant c_1 such that for two empirical distributions μ_n and ν_n with corresponding true distributions μ and ν , we have

$$\mathbb{E}[W_2^2(\mu_n, \nu_n)] \leq 3W_2^2(\mu, \nu) + \frac{6c_1}{n-j}.$$

This follows from this line of reasoning: Let $X^{(k)}$ and $Y^{(k)}$ denote the k -th order statistics of the samples from μ and ν respectively. Let F_μ^{-1} and F_ν^{-1} denote the quantile functions of μ and ν , respectively. Then, we have

$$\begin{aligned} &\mathbb{E}[W_2^2(\mu_n, \nu_n)] \\ &= \frac{1}{n} \sum_{k=1}^n \mathbb{E}\left[\left(X^{(k)} - Y^{(k)}\right)^2\right] \\ &= \sum_{k=1}^n \int_{(k-1)/n}^{k/n} \mathbb{E}\left[\left(X^{(k)} - F_\mu^{-1}(t) + F_\mu^{-1}(t) - F_\nu^{-1}(t) + F_\nu^{-1}(t) - Y^{(k)}\right)^2\right] dt \\ &\leq 3 \sum_{k=1}^n \int_{(k-1)/n}^{k/n} \mathbb{E}\left[\left(X^{(k)} - F_\mu^{-1}(t)\right)^2 + \left(F_\mu^{-1}(t) - F_\nu^{-1}(t)\right)^2 + \left(F_\nu^{-1}(t) - Y^{(k)}\right)^2\right] dt \\ &= 3W_2^2(\mu, \nu) + 3\mathbb{E}[W_2^2(\mu_n, \mu)] + 3\mathbb{E}[W_2^2(\nu_n, \nu)] \\ &\leq 3W_2^2(\mu, \nu) + \frac{6c_1}{n-j}. \end{aligned}$$

Then, let $\mathbb{E}[W_2^2(\mu_{ij}, \mu_{uj})] \leq \frac{\eta'}{3} - \frac{6c_1}{n-j}$. So, we get

$$\mathbb{E}[W_2^2(Y_{ij}, Y_{uj})] \leq \eta'.$$

Thus, we have that the bound on $\mathbb{E}[W_2^2(\mu_{ij}, \mu_{uj})]$ implies the bound on $\mathbb{E}[W_2^2(Y_{ij}, Y_{uj})]$. So, we have

$$\mathbb{P}\left(\mathbb{E}[W_2^2(\mu_{ij}, \mu_{uj})] \leq \frac{\eta'}{3} - \frac{6c_1}{n-j}\right) \leq \mathbb{P}(\mathbb{E}[W_2^2(Y_{ij}, Y_{uj})] \leq \eta').$$

Rewriting this in the ϕ and ψ notation, we have that

$$\phi\left(x_{\text{row}}^{(i)}, \frac{\eta'}{3} - \frac{6c_1}{n-j}\right) \leq \psi(x_{\text{row}}^{(i)}, \eta').$$

Thus, we obtain the first part of our claim. For the second part, we have

$$\begin{aligned} & \mathbb{P}\left(\rho_{iu} - \mathbb{E}_{\mathcal{H}_{\text{col}}}\left[\mathbb{E}\left[W_2^2(Y_{iv}, Y_{u_0v})\right]\right] > \eta - \eta' \mid x_{\text{row}}^{(i)}, |\Omega| \geq 1\right) \\ & \leq \mathbb{P}\left(\rho_{iu} - \mathbb{E}_{\mathcal{H}_{\text{col}}}\left[\mathbb{E}\left[W_2^2(Y_{iv}, Y_{u_0v})\right]\right] > \eta - \eta' \mid x_{\text{row}}^{(i)}, |\mathcal{C}_{iu}| \geq \frac{1}{2}Mp^2\right) \\ & \quad + \mathbb{P}\left(|\mathcal{C}_{iu}| < \frac{1}{2}Mp^2 \mid x_{\text{row}}^{(i)}\right) \\ & \leq \exp\left(-c \frac{(\eta - \eta')^2}{K^2} \frac{1}{2}Mp^2\right) + \exp\left(-\frac{Mp^2}{8}\right) \\ & \leq \exp(-2\log(N)) + \exp\left(-\frac{Mp^2}{8}\right) \\ & = \frac{1}{N^2} + \exp\left(-\frac{Mp^2}{8}\right) \end{aligned}$$

which completes the proof of our claim.

APPENDIX D: CONTINUOUS UNIFORM LOCATION-SCALE CASE

For the uniform distribution, the expected squared Wasserstein distance between an empirical distribution and its true distribution can be analytically derived. Let Θ denote asymptotic upper and lower bounds. From [10], we have for $\mu = \text{Unif}(0, 1)$ and μ_n being the empirical distribution of n samples from μ :

$$\mathbb{E}[W_2^2(\mu_n, \mu)] = \Theta\left(\frac{1}{n}\right)$$

and if we take the barycenter of m i.i.d. empirical distributions, then the expected squared Wasserstein distance between the Wasserstein barycenter of the empirical distributions and the true distribution is given in the following lemma:

LEMMA 5 (Expected error for the empirical barycenter of uniform distributions). *For $i = 1, \dots, m$, let $X_{1,i}, \dots, X_{n,i} \stackrel{\text{i.i.d.}}{\sim} \mu_i \triangleq \text{Unif}(a_i, b_i)$ and $\hat{\mu}_n^{(i)} \triangleq \frac{1}{n} \sum_{k=1}^n \delta_{X_{k,i}}$, for scalars a_i, b_i and $\bar{a} \triangleq \frac{\sum_{i=1}^m a_i}{m}$ and $\bar{b} \triangleq \frac{\sum_{i=1}^m b_i}{m}$. Let $\hat{\mu}$ and μ respectively denote the empirical barycenter and barycenter of the distributions $\{\hat{\mu}_n^{(i)}\}_{i=1}^m$ and $\{\mu_i\}_{i=1}^m$. Then, we have*

$$\mathbb{E}[W_2^2(\hat{\mu}, \mu)] = \frac{(\bar{b} - \bar{a})^2}{6m(n+1)} + \frac{(\bar{b} - \bar{a})^2}{6n(n+1)} = \Theta\left(\frac{1}{mn} + \frac{1}{n^2}\right),$$

where Big- Θ notation denotes both upper and lower rates.

D.1. Proof of Lem. 5. Let $X_i^{(k)}$ denote the k -th order statistic corresponding to distribution μ_i and $\bar{X}^{(k)} \triangleq \frac{1}{m} \sum_{i=1}^m X_i^{(k)}$. Now, we calculate the distribution of the barycenter

μ :

$$\begin{aligned} F_\mu^{-1}(t) &= \frac{1}{m} \sum_{i=1}^m F_{\mu_i}^{-1}(t) = \frac{1}{m} \sum_{i=1}^m [a_i + t(b_i - a_i)] \\ &= \left(\frac{1}{m} \sum_{i=1}^m a_i \right) + t \left(\frac{1}{m} \sum_{i=1}^m b_i - \frac{1}{m} \sum_{i=1}^m a_i \right). \end{aligned}$$

Let $\bar{a} = \frac{1}{m} \sum_{i=1}^m a_i$ and $\bar{b} = \frac{1}{m} \sum_{i=1}^m b_i$. Then, $\mu = \text{Unif}(\bar{a}, \bar{b})$. Next, from [8, Thm. 3.1] we have

$$\mathbb{E}[W_2^2(\hat{\mu}, \mu)] = \frac{1}{mn} \sum_{k=1}^n \text{Var}(\bar{X}^{(k)}) + \sum_{k=1}^n \int_{(k-1)/n}^{k/n} \left(\mathbb{E}[\bar{X}^{(k)}] - F_\mu^{-1}(t) \right)^2 dt.$$

Note that there is no leading term on the order of $O(1/m)$ like in [8, Thm. 3.1] because the barycenter of these distributions is equal to the “true” barycenter as described in [8] since our true barycenter is the empirical average of our given distributions (i.e. the barycenter itself). Next, we have

$$\frac{1}{mn} \sum_{k=1}^n \text{Var}(\bar{X}^{(k)}) = \frac{(\bar{b} - \bar{a})^2}{mn} \sum_{k=1}^n \frac{k(n-k+1)}{(n+1)^2(n+2)} \stackrel{(a)}{=} \frac{(\bar{b} - \bar{a})^2}{6m(n+1)},$$

where (a) follows from the proof of Theorem 4.7 in [10]. Finally, we have

$$\begin{aligned} \sum_{k=1}^n \int_{(k-1)/n}^{k/n} \left(\mathbb{E}[\bar{X}^{(k)}] - F_\mu^{-1}(t) \right)^2 dt &= (\bar{b} - \bar{a})^2 \sum_{k=1}^n \int_{(k-1)/n}^{k/n} \left(\frac{k}{n+1} - t \right)^2 dt \\ &\stackrel{(a)}{=} (\bar{b} - \bar{a})^2 \left(\frac{1}{6n} - \frac{1}{6(n+1)} \right) \\ &= \frac{(\bar{b} - \bar{a})^2}{6n(n+1)}, \end{aligned}$$

where (a) follows again from Theorem 4.7 in [10]. Putting these together, we recover the result in Eq. (3.3) in [8]:

$$\mathbb{E}[W_2^2(\hat{\mu}, \mu)] = \Theta\left(\frac{1}{mn} + \frac{1}{n^2}\right).$$

LEMMA 6. Let $\mu = \text{Unif}(a, b)$ and $\nu = \text{Unif}(c, d)$. Then, we have

$$W_2^2(\mu, \nu) = \frac{1}{3} \left[(a-c)^2 + (b-d)^2 + (a-c)(b-d) \right].$$

PROOF. From the definition of the 2-Wasserstein metric, we have

$$\begin{aligned} W_2^2(\mu, \nu) &= \int_0^1 (F_\mu^{-1}(t) - F_\nu^{-1}(t))^2 dt = \int_0^1 (a + (b-a)t - c - (d-c)t)^2 dt \\ &= \frac{1}{3} \left[(a-c)^2 + (b-d)^2 + (a-c)(b-d) \right], \end{aligned}$$

which is the desired claim. \square

LEMMA 7. Let $X_1, \dots, X_n \stackrel{\text{i.i.d.}}{\sim} \mu \triangleq \text{Unif}(a, b)$, and let $\mu_n \triangleq \frac{1}{n} \sum_{i=1}^n \delta_{X_i}$ denote the empirical measure. Then, we have

$$(39) \quad \mathbb{E}[W_2^2(\mu_n, \mu)] = \frac{(b-a)^2}{6n}.$$

Furthermore, if let $Y_1, \dots, Y_n \stackrel{\text{i.i.d.}}{\sim} \nu \triangleq \text{Unif}(c, d)$ with $\nu_n \triangleq \frac{1}{n} \sum_{i=1}^n \delta_{Y_i}$, then we have

$$(40) \quad \mathbb{E}[W_2^2(\mu_n, \nu_n)] = W_2^2(\mu, \nu) + \frac{(b-a)(d-c)}{3(n+1)}.$$

PROOF. We utilize identities from the proof of Theorem 4.7 in [10]. We know that for $U_1, \dots, U_n \sim \text{Unif}(0, 1)$, their k -th order statistic $U^{(k)}$ satisfies a $\text{Beta}(k, n-k+1)$ distribution. So, we have

$$\mathbb{E}[U^{(k)}] = \frac{k}{n+1}, \quad \text{and} \quad \text{Var}(U^{(k)}) = \frac{k(n-k+1)}{(n+1)^2(n+2)}.$$

And hence, for the k -th order statistic of (X_1, \dots, X_n) , denoted by $X^{(k)}$, we have

$$(41) \quad \mathbb{E}[X^{(k)}] = \mathbb{E}\left[a + (b-a)U^{(k)}\right] = a + (b-a)\frac{k}{n+1} \quad \text{and}$$

$$(42) \quad \text{Var}(X^{(k)}) = \text{Var}\left(a + (b-a)U^{(k)}\right) = (b-a)^2 \frac{k(n-k+1)}{(n+1)^2(n+2)}.$$

Putting these together and using [10, Cor. 4.5], we find that

$$\begin{aligned} \mathbb{E}[W_2^2(\mu_n, \mu)] &= \frac{1}{n} \sum_{k=1}^n \text{Var}(X^{(k)}) + \sum_{k=1}^n \int_{(k-1)/n}^{k/n} \left(\mathbb{E}[X^{(k)}] - F_\mu^{-1}(t)\right)^2 dt \\ &= \frac{1}{n} \sum_{k=1}^n \frac{(b-a)^2 k(n-k+1)}{(n+1)^2(n+2)} \\ &\quad + \sum_{k=1}^n \int_{(k-1)/n}^{k/n} \left(a + (b-a)\frac{k}{n+1} - a - (b-a)t\right)^2 dt \\ &= (b-a)^2 \frac{1}{n} \sum_{k=1}^n \frac{k(n-k+1)}{(n+1)^2(n+2)} + (b-a)^2 \sum_{k=1}^n \int_{(k-1)/n}^{k/n} \left(\frac{k}{n+1} - t\right)^2 dt \\ &= \frac{(b-a)^2}{6n}, \end{aligned}$$

which yields the first claim (39). To prove the second claim (40), using the equalities (41) and (42), we find that

$$\begin{aligned} \mathbb{E}[W_2^2(\mu_n, \nu_n)] &\stackrel{(4)}{=} \frac{1}{n} \sum_{k=1}^n \mathbb{E}\left[\left(X^{(k)} - Y^{(k)}\right)^2\right] \\ &= \frac{1}{n} \sum_{k=1}^n \left[\mathbb{E}\left[\left(X^{(k)}\right)^2\right] + \mathbb{E}\left[\left(Y^{(k)}\right)^2\right] - 2\mathbb{E}[X^{(k)}]\mathbb{E}[Y^{(k)}]\right] \\ &= \frac{1}{n} \sum_{k=1}^n \left[\text{Var}(X^{(k)}) + \text{Var}(Y^{(k)}) + \left(\mathbb{E}[X^{(k)}] - \mathbb{E}[Y^{(k)}]\right)^2\right] \end{aligned}$$

$$= \frac{(b-a)^2 + (d-c)^2}{6(n+1)} + \frac{1}{n} \sum_{k=1}^n \left(\mathbb{E}[X^{(k)}] - \mathbb{E}[Y^{(k)}] \right)^2.$$

Next, we have

$$\begin{aligned} & \frac{1}{n} \sum_{k=1}^n \left(\mathbb{E}[X^{(k)}] - \mathbb{E}[Y^{(k)}] \right)^2 \\ &= \frac{1}{n} \sum_{k=1}^n \left[a + (b-a) \frac{k}{n+1} - \left(c + (d-c) \frac{k}{n+1} \right) \right]^2 \\ &= \frac{1}{n} \sum_{k=1}^n \left[(a-c) + ((b-a) - (d-c)) \frac{k}{n+1} \right]^2 \\ &= \frac{1}{n} \sum_{k=1}^n \left[(a-c)^2 + 2(a-c)((b-a) - (d-c)) \frac{k}{n+1} + ((b-a) - (d-c))^2 \frac{k^2}{(n+1)^2} \right] \\ &= (a-c)^2 + \frac{2(a-c)((b-a) - (d-c))}{n(n+1)} \left(\sum_{k=1}^n k \right) + \frac{((b-a) - (d-c))^2}{n(n+1)^2} \left(\sum_{k=1}^n k^2 \right) \\ &= (a-c)^2 + \frac{2(a-c)((b-a) - (d-c))}{n(n+1)} \cdot \frac{n(n+1)}{2} \\ &\quad + \frac{((b-a) - (d-c))^2}{n(n+1)^2} \cdot \frac{n(n+1)(2n+1)}{6} \\ &= (a-c)^2 + (a-c)((b-a) - (d-c)) + \frac{((b-a) - (d-c))^2(2n+1)}{6(n+1)} \\ &= (a-c)(b-d) + \frac{((b-a) - (d-c))^2(2n+1)}{6(n+1)}. \end{aligned}$$

Putting these together, we obtain

$$\begin{aligned} & \mathbb{E}[W_2^2(\mu_n, \nu_n)] \\ &= \frac{(b-a)^2 + (d-c)^2}{6(n+1)} + \frac{1}{n} \sum_{k=1}^n \left(\mathbb{E}[X^{(k)}] - \mathbb{E}[Y^{(k)}] \right)^2 \\ &= \frac{(b-a)^2 + (d-c)^2}{6(n+1)} + (a-c)(b-d) + \frac{((b-a) - (d-c))^2(2n+1)}{6(n+1)} \\ &= \frac{((b-a) - (d-c))^2}{3} + (a-c)(b-d) + \frac{(b-a)(d-c)}{3(n+1)} \\ &= \frac{1}{3} \left[(a-c)^2 + (b-d)^2 + (a-c)(b-d) \right] + \frac{(b-a)(d-c)}{3(n+1)} \\ &= W_2^2(\mu, \nu) + \frac{(b-a)(d-c)}{3(n+1)}, \end{aligned}$$

as claimed. \square

Acknowledgments. The corresponding author for this paper is Jacob Feitelberg. The authors would like to thank the anonymous referees, the Associate Editor, and the Editor for their constructive comments that improved the quality of this paper.

Funding. Jacob Feitelberg and Anish Agarwal’s work on this paper was supported by the Columbia Center for AI and Responsible Financial Innovation in collaboration with Capital One.

REFERENCES

- [1] ABADIE, A. (2021). Using Synthetic Controls: Feasibility, Data Requirements, and Methodological Aspects. *Journal of Economic Literature* **59** 391–425. <https://doi.org/10.1257/jel.20191450>
- [2] ADLER, R. J. and TAYLOR, J. E. (2009). *Random fields and geometry*. Springer Science & Business Media.
- [3] AGARWAL, A., DAHLEH, M., SHAH, D. and SHEN, D. (2023). Causal matrix completion. In *The Thirty Sixth Annual Conference on Learning Theory* 3821–3826. PMLR.
- [4] ALTSCHULER, J. M. and BOIX-ADSERA, E. (2022). Wasserstein barycenters are NP-hard to compute. *SIAM Journal on Mathematics of Data Science* **4** 179–203.
- [5] BERGSTRA, J., BARDENET, R., BENGIO, Y. and KÉGL, B. (2011). Algorithms for hyper-parameter optimization. *Advances in neural information processing systems* **24**.
- [6] BIGOT, JÉRÉMIE (2020). Statistical data analysis in the Wasserstein space*. *ESAIM: ProcS* **68** 1–19.
- [7] BIGOT, J., GOUET, R., KLEIN, T. and LÓPEZ, A. (2017). Geodesic PCA in the Wasserstein space by convex PCA. *Annales de l’Institut Henri Poincaré, Probabilités et Statistiques* **53** 1 – 26.
- [8] BIGOT, J., GOUET, R., KLEIN, T. and LÓPEZ, A. (2018). Upper and lower risk bounds for estimating the Wasserstein barycenter of random measures on the real line. *Electronic Journal of Statistics* **12** 2253 – 2289.
- [9] BIGOT, J., KLEIN, T. et al. (2012). Consistent estimation of a population barycenter in the Wasserstein space. *ArXiv e-prints* **49**.
- [10] BOBKOV, S. and LEDOUX, M. (2019). *One-dimensional empirical measures, order statistics, and Kantorovich transport distances* **261**. American Mathematical Society.
- [11] CAI, T. T. and ZHOU, W.-X. (2013). Matrix Completion via Max-Norm Constrained Optimization. *arXiv preprint arXiv:1303.0341*.
- [12] CANDÈS, E. J. and PLAN, Y. (2010). Matrix Completion With Noise. *Proceedings of the IEEE* **98** 925–936. <https://doi.org/10.1109/JPROC.2009.2035722>
- [13] CAROTHERS, N. L. (2000). *Real analysis*. Cambridge University Press.
- [14] CHATTERJEE, S. (2015). MATRIX ESTIMATION BY UNIVERSAL SINGULAR VALUE THRESHOLDING. *The Annals of Statistics* **43** 177–214.
- [15] CHEN, Y., GEORGIU, T. T. and PAVON, M. (2021). Optimal transport in systems and control. *Annual Review of Control, Robotics, and Autonomous Systems* **4** 89–113.
- [16] CHI, Y. (2018). Low-rank matrix completion [lecture notes]. *IEEE Signal Processing Magazine* **35** 178–181.
- [17] CHIN, C., KHUBCHANDANI, A., MASKARA, H., CHOI, K., FEITELBERG, J., GONG, A., PAUL, M., SADHUKHAN, T., AGARWAL, A. and DWIVEDI, R. (2025). N^2 : A Unified Python Package and Test Bench for Nearest Neighbor-Based Matrix Completion.
- [18] CORMEN, T. H., LEISERSON, C. E., RIVEST, R. L. and STEIN, C. (2022). *Introduction to algorithms*. MIT press.
- [19] CSORGO, M. and RÉVÉSZ, P. (1978). Strong approximations of the quantile process. *The Annals of Statistics* 882–894.
- [20] CUTURI, M. and DOUCET, A. (2014). Fast Computation of Wasserstein Barycenters. In *Proceedings of the 31st International Conference on Machine Learning* (E. P. XING and T. JEBARA, eds.). *Proceedings of Machine Learning Research* **32** 685–693. PMLR, Beijing, China.
- [21] DOU, Y., YANG, H. and DENG, X. (2016). A survey of collaborative filtering algorithms for social recommender systems. In *2016 12th International conference on semantics, knowledge and grids (SKG)* 40–46. IEEE.
- [22] DU, R., CHEN, C., YANG, B. and GUAN, X. (2013). Vanet based traffic estimation: A matrix completion approach. In *2013 IEEE Global Communications Conference (GLOBECOM)* 30–35. IEEE.
- [23] DU, R., CHEN, C., YANG, B., LU, N., GUAN, X. and SHEN, X. (2015). Effective Urban Traffic Monitoring by Vehicular Sensor Networks. *IEEE Transactions on Vehicular Technology* **64** 273–286. <https://doi.org/10.1109/TVT.2014.2321010>

- [24] DWIVEDI, R., TIAN, K., TOMKINS, S., KLASNJA, P., MURPHY, S. and SHAH, D. (2022). Counterfactual inference for sequential experiments. *arXiv preprint arXiv:2202.06891*.
- [25] DWIVEDI, R., TIAN, K., TOMKINS, S., KLASNJA, P., MURPHY, S. and SHAH, D. (2022). Doubly robust nearest neighbors in factor models. *arXiv preprint arXiv:2211.14297*.
- [26] FEYDY, J., CHARLIER, B., VIALARD, F.-X. and PEYRÉ, G. (2017). Optimal transport for diffeomorphic registration. In *Medical Image Computing and Computer Assisted Intervention- MICCAI 2017: 20th International Conference, Quebec City, QC, Canada, September 11-13, 2017, Proceedings, Part I* 20 291–299. Springer.
- [27] FOURNIER, N. and GUILLIN, A. (2015). On the rate of convergence in Wasserstein distance of the empirical measure. *Probability theory and related fields* **162** 707–738.
- [28] GARSIA, A. M., RODEMICH, E., RUMSEY, H. and ROSENBLATT, M. (1970). A real variable lemma and the continuity of paths of some Gaussian processes. *Indiana University Mathematics Journal* **20** 565–578.
- [29] GUNSILIUS, F. F. (2023). Distributional synthetic controls. *Econometrica* **91** 1105–1117.
- [30] HARDY, G. H., LITTLEWOOD, J. E. and PÓLYA, G. (1952). *Inequalities*. Cambridge university press.
- [31] KANG, Z., PENG, C. and CHENG, Q. (2016). Top-n recommender system via matrix completion. In *Proceedings of the AAAI conference on artificial intelligence* **30**.
- [32] KHAN, B. M., MANSHA, A., KHAN, F. H. and BASHIR, S. (2017). Collaborative filtering based online recommendation systems: A survey. In *2017 International Conference on Information and Communication Technologies (ICICT)* 125–130. IEEE.
- [33] KOLOURI, S., PARK, S. R., THORPE, M., SLEPCEV, D. and ROHDE, G. K. (2017). Optimal mass transport: Signal processing and machine-learning applications. *IEEE signal processing magazine* **34** 43–59.
- [34] LE GOUIC, T., PARIS, Q., RIGOLLET, P. and STROMME, A. J. (2022). Fast convergence of empirical barycenters in Alexandrov spaces and the Wasserstein space. *Journal of the European Mathematical Society* **25** 2229–2250.
- [35] LI, Y., SHAH, D., SONG, D. and YU, C. L. (2019). Nearest neighbors for matrix estimation interpreted as blind regression for latent variable model. *IEEE Transactions on Information Theory* **66** 1760–1784.
- [36] LIU, Z. and VANDENBERGHE, L. (2010). Interior-point method for nuclear norm approximation with application to system identification. *SIAM Journal on Matrix Analysis and Applications* **31** 1235–1256.
- [37] MARTINET, G. G., STRZALKOWSKI, A. and ENGELHARDT, B. (2022). Variance minimization in the wasserstein space for invariant causal prediction. In *International Conference on Artificial Intelligence and Statistics* 8803–8851. PMLR.
- [38] MONGE, G. (1781). *Mémoire sur la théorie des déblais et des remblais*. De l’Imprimerie Royale.
- [39] NGUYEN, L. T., KIM, J., KIM, S. and SHIM, B. (2019). Localization of IoT networks via low-rank matrix completion. *IEEE Transactions on Communications* **67** 5833–5847.
- [40] PAPP, T. and SHERLOCK, C. (2022). Bounds on Wasserstein distances between continuous distributions using independent samples. *arXiv preprint arXiv:2203.11627*.
- [41] RAMLATCHAN, A., YANG, M., LIU, Q., LI, M., WANG, J. and LI, Y. (2018). A survey of matrix completion methods for recommendation systems. *Big Data Mining and Analytics* **1** 308–323.
- [42] ROSS, S. M. (1995). *Stochastic processes*. John Wiley & Sons.
- [43] SHORACK, G. R. and WELLNER, J. A. (2009). *Empirical processes with applications to statistics*. SIAM.
- [44] SOLEYMANI, M., LIU, Q., MAHDAVIFAR, H. and BALZANO, L. (2023). Matrix Completion over Finite Fields: Bounds and Belief Propagation Algorithms. In *2023 IEEE International Symposium on Information Theory (ISIT)* 1166–1171. IEEE.
- [45] SU, X. and KHOSHGOFTAAR, T. M. (2009). A survey of collaborative filtering techniques. *Advances in artificial intelligence* **2009**.
- [46] THORPE, M. (2018). Introduction to optimal transport. *Notes of Course at University of Cambridge*.
- [47] VERSHYNIN, R. (2020). High-dimensional probability. *University of California, Irvine*.
- [48] WASKOM, M. L. (2021). seaborn: statistical data visualization. *Journal of Open Source Software* **6** 3021. <https://doi.org/10.21105/joss.03021>
- [49] WASSERMAN, L. (2017). Optimal transport and Wasserstein distance.
- [50] WEISSTEIN, E. W. (2004). Bonferroni correction. <https://mathworld.wolfram.com/>.
- [51] XIE, K., LI, X., WANG, X., XIE, G., WEN, J. and ZHANG, D. (2019). Active sparse mobile crowd sensing based on matrix completion. In *Proceedings of the 2019 international conference on management of data* 195–210.
- [52] YANG, S., KALPAKIS, K., MACKENZIE, C. F., STANSBURY, L. G., STEIN, D. M., SCALEA, T. M. and HU, P. F. (2012). Online recovery of missing values in vital signs data streams using low-rank matrix completion. In *2012 11th International Conference on Machine Learning and Applications* **1** 281–287. IEEE.

- [53] ZHOU, H., ZHANG, D. and XIE, K. (2017). Accurate traffic matrix completion based on multi-Gaussian models. *Computer Communications* **102** 165–176.